189

POROSITY AND CEMENT DEVELOPMENT IN PLEISTOCENE KEY LARGO LIMESTONE, KEY LARGO FLORIDA

POROSITY AND CEMENT DEVELOPMENT IN PLEISTOCENE KEY LARGO LIMESTONE, KEY LARGO FLORIDA

By

LORIE DEBRA COOPER

A Thesis
Submitted to the Department of Geology
in Partial Fulfilment of the Requirements
for the Degree
Bachelor of Science

McMaster University
May, 1982

BACHELOR OF SCIENCE (1982) McMASTER UNIVERSITY
(Geology) Hamilton, Ontario

TITLE: Porosity and Cement Development in Pleistocene Key Largo Limestone, Key Largo Florida

AUTHOR: Lorie Debra Cooper

SUPERVISOR: Dr. Michael J. Risk

NUMBER OF PAGES: vii, 53,v, J

ABSTRACT

A detailed petrographic study of the Pleistocene Key Largo Limestone Formation, Key Largo, Florida, was undertaken observing three units of varying ages. From oldest to youngest, these are: Q4A, (age unknown); Q4B, (180,000 years B.P.), and Q5, (125,000 years B.P.). Fifty thin sections from four cored wells were point counted. Porosity remained constant for all three units at 28.5% as did total cements at 27.5%. These are still very porous rocks relative to ancient carbonates, which generally show 0-2% porosity. Q5 is diagenetically less mature than Q4B and Q4A, with the persistence of aragonite (which is being leached) and solution-enhanced interparticle porosity. Q5 has been exposed to a vadose environment. Multiple generation cements in Q4B indicate two periods of vadose exposure coincident with known Pleistocene eustatic sea level fluctuations. Moldic porosity is predominant in Q4B. Vague horizons of macroscopic vuggy porosity act as pathways of directed flow for percolating fluids precipitating late stage cements and stains rich in iron. Q4A has been interpreted as a beachrock in part, deposited at pH's greater than 9, resulting in dissolution of quartz grains. Of special interest in Q4A is the probable exploitation of a quartz substrate by endolithic borers.

ACKNOWLEDGEMENTS

I am indebted to Dr. Michael Risk of McMaster University, for financial support and supervision. A special thanks to Dr. Rand Harrison of the Alberta Research Council for suggesting the project, providing thin sections and core, and for invaluable comments and encouragement. Research facilities were generously made available by the Alberta Research Council in the initial stages of the project, the University of Manitoba geology department, and McMaster University geology department.

Photographic services rendered by Jack Whorwood, and the typing of the manuscript by Libby Ginn are deeply appreciated. I would like to acknowledge the helpful input from professors and colleagues at McMaster University throughout the project.

TABLE OF CONTENTS

LIST OF ILLUSTRATIONS

LIST OF PLATES

1. INTRODUCTION

Much of the carbonate literature deals with modern or ancient carbonate examples. The Pleistocene carbonates of Key Largo offer a unique opportunity to study carbonates of an intermediate age for which sea level fluctuations are partially known. The purpose of this study is to compare and contrast the development of porosity and cements for three carbonate units Q4A, Q4B and Q5, of varying ages from the Pleistocene Key Largo Limestone, Key Largo Florida. Main body diagenesis, rather than subaerial effects associated with regional discontinuity surfaces, will be studied.

Regional Setting

The Florida Keys form an arcuate discontinuous chain of islands extending 280 km. from the southern tip of Florida (Fig. 1). To the east, 6-10 km., is the present day reef tract with a similar orientation as the Keys. The reef slopes dramatically to the Straits of Florida with depths of 800-1,000 m (Bathurst, 1976). Along the eastern Florida shoreline, an intermittent countercurrent flows towards the south transporting minor amounts of clastic debris via longshore drift. Florida Bay lies immediately west of the Keys, an area of 3,500 m^2, mostly floored with lime mud (Bathurst, 1976). The climate is subtropical with

an average temperature at 22.5°C. The Pleistocene climate of this area is believed to have been similar. The rainfall is 152 cm. per year, 75% of which falls during June to October, the hurricane season. Southeasterly trade winds and storms effectively flush marine water through the porous Keys.

Of specific interest for this project is Key Largo, the northern-most Key, 46 km. x 0.5-3.6 km., aligned in a north-south direction. There is no evidence to support the existence of a permanent freshwater phreatic lens on Key Largo (Harrison, person. commun.). The surface rock of the upper Keys, including Key Largo, is the "Key Largo Limestone" of Pleistocene age first described and named by Sanford, 1909 (Stanley, 1966 p.1927). The Pleistocene in southern Florida was a period of minimal tectonic activity (Perkins, 1977).

Previous Work

Stanley (1966) described the exposed Upper Key Largo Limestone Formation at two locations: Windley Key Quarry on Windley Key and exposures along the man-made waterway on Key Largo (PLATE 1). The later location is coincident with one of four cored sections used for this study. The limestone was described as 30% *in situ* organic framework composed of hermatypic corals. *Montastrea*

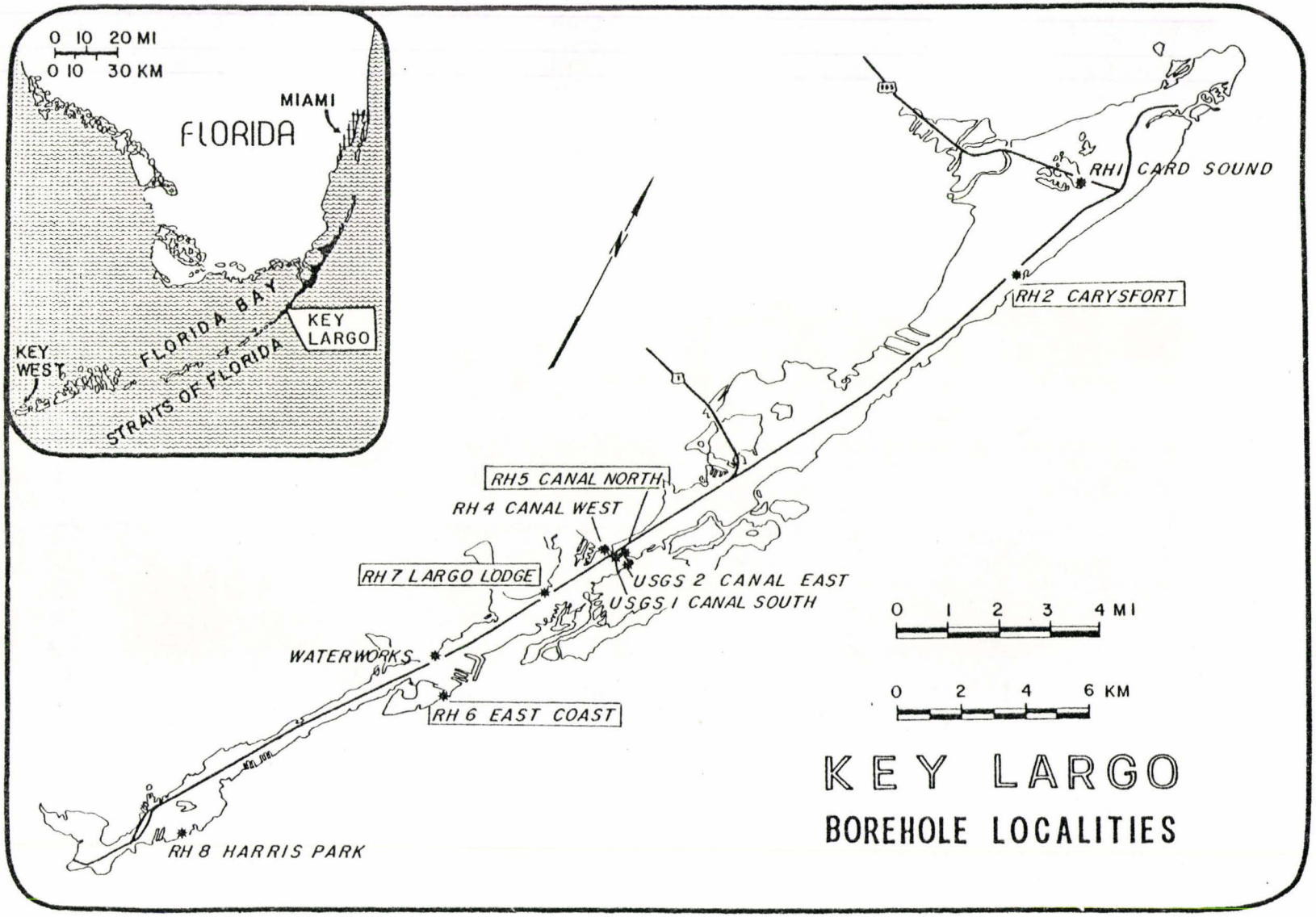

Figure 1. (modified from Harrison, unpub.)

PLATE I

Upper Key Largo Limestone, Unit Q5,
exposed along Key Largo Waterway,
Key Largo, Florida

annularis is the most abundant coral, with lesser abundances of Porites astreoides, Diploria strigosa, Diploria clivosa and Diploria labyrinthiformis. Based on his observations, Stanley proposed two hypotheses for the origin of the Keys. The conspicuous absence of Acropora palmata, a high energy surf zone coral found in abundance on the present reef-tract, led him to believe that the Keys were coalescing patch reefs in a quieter environment located behind a windward bank reef. Stanley's alternative hypothesis suggests that the Keys were the main component of the reef at depths of 6.1m-12.2m, much deeper than the present day reef tract. This hypothesis was based on the abundance of massive colonies of Montastrea annularis, a deeper water coral. From petrographic study of the Upper Key Largo Limestone Stanley (1966) concluded that aragonite was actively being dissolved while Mg-calcite was replaced early by stable low Mg-calcite.

Hoffmeister and Multer (1968) support the shallow water coalescing back reef-patch reef hypothesis for the origin of the Keys. Their studies revealed the thickness variation of the Key Largo Limestone on Key Largo, the northern portion having a thickness of 44.2 m, a central thickness of 22.9 m, and the southern tip 30.5 m.

More recently Perkins (1977) recognized 5 units,

Q1 to Q5, representing oldest to youngest units, in a regional stratigraphic study of South Florida based on 56 measured sections. The units were defined by regional discontinuity surfaces that are time stratigraphic, displaying distinct subaerial fabrics. The carbonate units represent periods of high eustatic sea level and the discontinuity surfaces periods of low sea level (Perkins', 1977). Broeker and Thurber (1965) determined an age of 120-130,000 years for a horizon coincident with Perkins Q5 unit, using radiometric dating. Mitterer (1975) determined the ages for five units coincident with Perkins Q1-Q5 units. Mitterer's dates were calculated using the epimerization reaction of isoleucine within the carbonate test of Mercenaria. The ages are: I. no absolute, II(Q2) 324,000 years, III.(Q3) 236,000 years, IV.(Q4) 180,000 years, and V.(Q5) 134,000 years (Mitterer, 1975).

"Considered as a whole the Pleistocene record of South Florida may be thought of as a simple infilling of pre-Pleistocene paleotopography during repeated marine transgressions, modified by subaerial exposure and the production of discontinuity surfaces during low sea level stands" (Perkins, 1977, p. 133).

Q4 can be further subdivided into Q4A/Q4B on the basis of a lithologic change and the presence of subaerial

fabrics suggesting a discontinuity surface (Harrison, person. commun.). Q4A is a clastic quartz bearing unit, and Q4B an overlying carbonate unit.

Coniglio's (1980) study of units Q3, Q4 and Q5 on Big Rine Key, in Southern Florida revealed that the principle diagenetic environment was vadose.

Samples

Ten wells were cored along the length of Key Largo in a drilling program conducted by R.S. Harrison in affiliation with the U.S. Geological Survey in 1978 (Fig. 1). Four wells and 94 corresponding thin sections were selected for a petrographic study of porosity and cement development in units Q4A, Q4B and Q5 of the Pleistocene Key Largo Limestone, Key Largo Florida. The wells are parallel to the strike of facies change, therefore they do not represent a progressional cross-section through varying facies. The wells RH-2, RH-5, RH-6 and RH-7 were selected because they were cored to the Q3 surface, have a high % recovery (Fig. 2), and transverse the length of the Key. Samples were taken at intervals along the 2" cores, to conduct a series of tests involving staining, scanning electron microscopy and x-ray diffraction analysis.

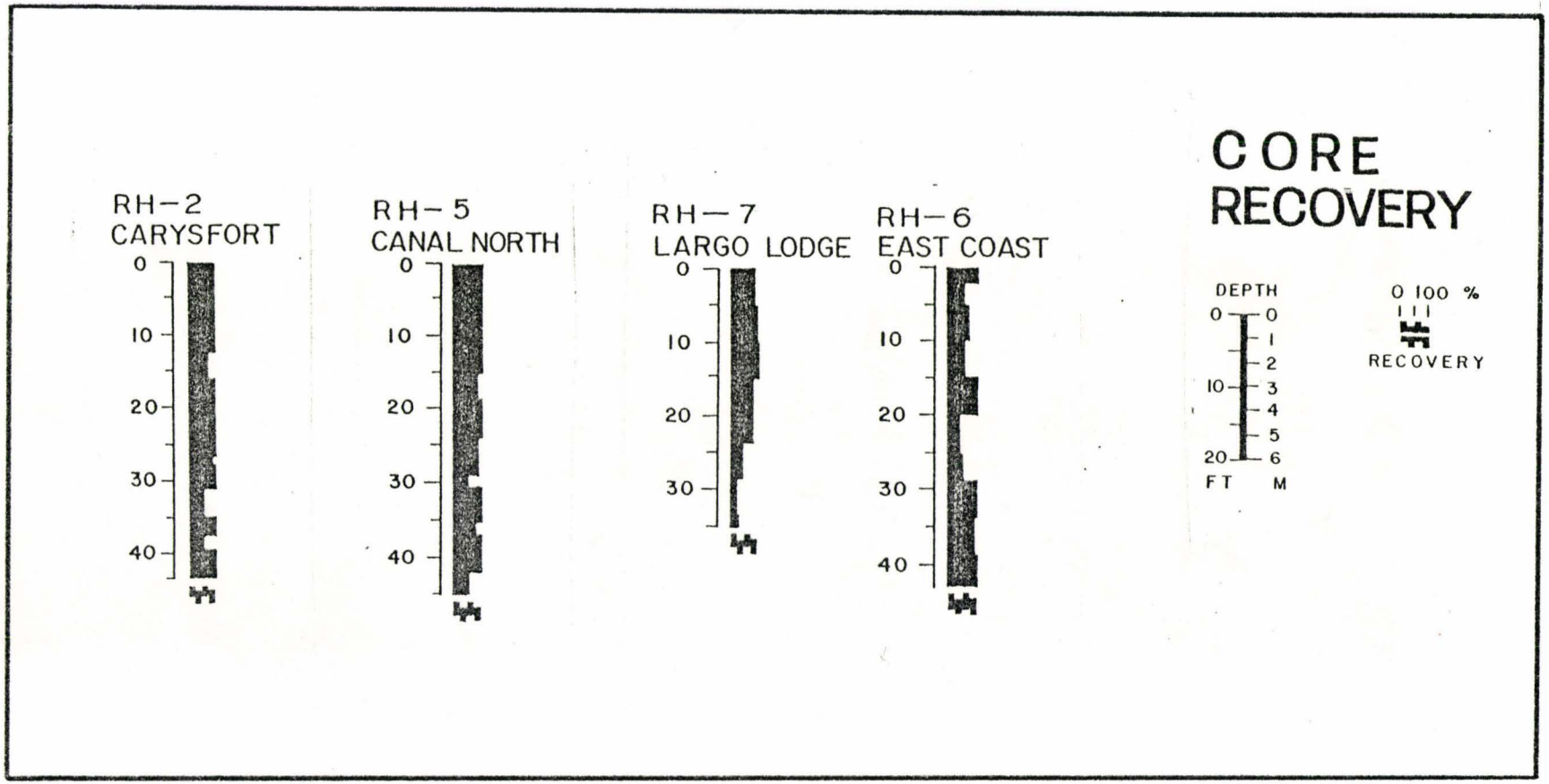

Figure 2. % Core Recovery (modified from Harrison, unpub.)

Methods

A total of 50 slides was point counted, 300 counts per slide at regular intervals delineating the relative percentages of grains, matrix, primary porosity, secondary porosity, calcite spar cement, micrite cement and micrite envelopes (Appendix A). The point counting was conducted at 10 magnification. Slides were selected at 0.6-0.9 meters from the discontinuity surfaces to avoid the immediate effects of subaerial diagenesis. The purpose of this study is to describe and interpret the "main body" diagenesis of these carbonate units.

Detailed descriptive petrography was done for RH-2, RH-5 and to a lesser extent for RH-6 and RH-7 using a polarizing microscope and the scanning electron microscope where applicable. The 2" diameter cores were logged and described to complement the microscopic study.

Twenty-one samples from RH-5 and RH-2 were stained using alizarin red and potassium ferrocyanide to differentiate calcite and ferroan calcite cements.

The quartz bearing Q4A unit suggested the existence of borings in the quartz grains. The quartz grains were removed from the carbonate matrix by immersing in a 10% HCl solution, then mounted on SEM stubs or embedded in spur resin.

2. SUBAERIAL DIAGENETIC FABRICS

For this study "main body" diagenesis is the primary concern. The effects of subaerial diagenesis will, however, be considered briefly. The recognition of subaerial surfaces has permitted the Key Largo Limestone formation to be subdivided into units of different histories and ages (Perkins, 1977). The discontinuity surfaces are distinguished by characteristic subaerial fabrics. These are: the development of caliche horizons, laminated crusts, paleosols, reddish-brown micrite in localized pockets, the presence of root pathways, solution pits, karst topography and solution breccias (Perkins 1977, Harrison and Steinen 1978). One or more of these features may be present. Such horizons tend to be better cemented near the surface, with diverse carbonate cement morphologies (Harrison and Steinen 1978). In the upper vadose zone supersaturation due to temperature increases, and evaporation results in rapid precipitation of carbonate cements from supersaturated solutions (Harrison 1977 in Coniglio p. 137). For a more detailed account of subaerial cementation mechanisms refer to Harrison, 1977.

The present day subaerial surface topping unit Q5 on the Keys ranges from less than 1 cm to 6 cm in thickness

(Multer and Hoffmeister, 1968). Bulk radiocarbon dating shows dates of 880 to 4395 ± 90 years for the age of formation of this Q5 surface (Multer and Hoffmeister, 1968). The present day Q5 surface and the Q4A/Q3 break (PLATE XII, Fig. 6) are distinguished by reddish-brown laminated surfaces (PLATE XIII, Fig. A). The breaks defining Q4A/Q4B and Q4B/Q5 are subtle with vague horizons defined by pockets of micrite and root fabrics (PLATE II, Fig. A), no discrete breaks occur. The reddish-brown coloration of the micrite and laminated crusts can be attributed to the presence of iron (Perkins 1977 p. 147). Each unit tends to be better cemented near the surface due to subaerial processes. Within Q5 subaerial fabrics (pockets of micrite, root channels), are macroscopically evident in core to depths of 0.8 m-1.5m below the laminated surface. A root pathway, 3 mm diameter, with an intact root was observed in RH-7 at a depth of 30.5 cm.

Abundant calcified tubules in close proximity to root pathways partially obscure the identity of the grains. These tubules have a diameter 10-20 μm's and are random in orientation. Occasionally, a spoke-like arrangement was observed, a circular tubule with tubules radiating from it. Coniglio observed similar networks (Coniglio, 1980). The origin of these structures is unclear. They have been

variously attributed to blue green algae sheaths (James 1972 in Coniglio), as having a terrestrial algal origin associated with roots (Harrison, person. commun.) and to the presence of calcified root hairs (Klappa, 1979). Remnant outlines of grains suggest that alteration of grains to localized patches of micrite near root pathways, was a secondary process associated with the presence of these tubules.

3. UNIT Q5

Observations

I. Grains

The thickness of the Q5 unit varies from 4.9 meters at RH-2 to a minimum thickness of 1.7 meters at RH-7. The Q5 unit is a fine to medium grain bioclastic packstone (Dunham, 1962),(PLATE II, Fig. D). Locally this may vary from a mud supported wackestone near the subaerial surface to a grainstone. Point counting reveals an average 29.7% grain content for Q5 with 14.8% matrix some of which is subaerial even though subaerial fabrics were avoided where possible. The grain constituents are hermatypic corals, the green alga Halimeda, molluscs, foraminifera, coralline algae and encrusting bryozoans. Coral fragments and Halimeda plates are the most common grains. Grains alter in a way that reflects the mineralogy of the grain.

Halimeda plates are light brown, elongate, aragonite plates, 1.6 x 0.3 mm, perforated with 30-50 µm utricles (PLATE III, Fig. B). Near the Q5 surface, at 0.61 m, these plates remain partially intact. The utricles are often rimmed with cryptocrystalline micrite cement, 10-15 µm thickness, which refracts a greyish brown color.

PLATE II Q5

Fig. A: RH-5, @ 1' (.3m)
Random pockets of reddish-brown subaerial micrite flushed into a Halimeda rich packstone from the Q5 surface. (scale is in 1cm increments)

Fig. B: RH-2, @ 5'5" (1.7m)
Can see primary shelter porosity and enhanced dissolution around mollusc fragments in Q5. The fine to medium matrix here is characteristic of Q5.

Fig. C: RH-2, @ 5' (1.5m)
Zone of dissolution and enhanced porosity on the underside of coral fragment. During compaction, the fine to med-grain matrix may have settled away from contact with the coral resulting in directed flow of solution waters and subsequent dissolution.

Fig. D: RH-5, slide #4 @ 5' (1.5m)
Preferential cementation of calcite spar occurs at grain contacts, and intergranular porosity remains open. Note the infilling of the inner chambers of the miliolid foram, lower left corner.

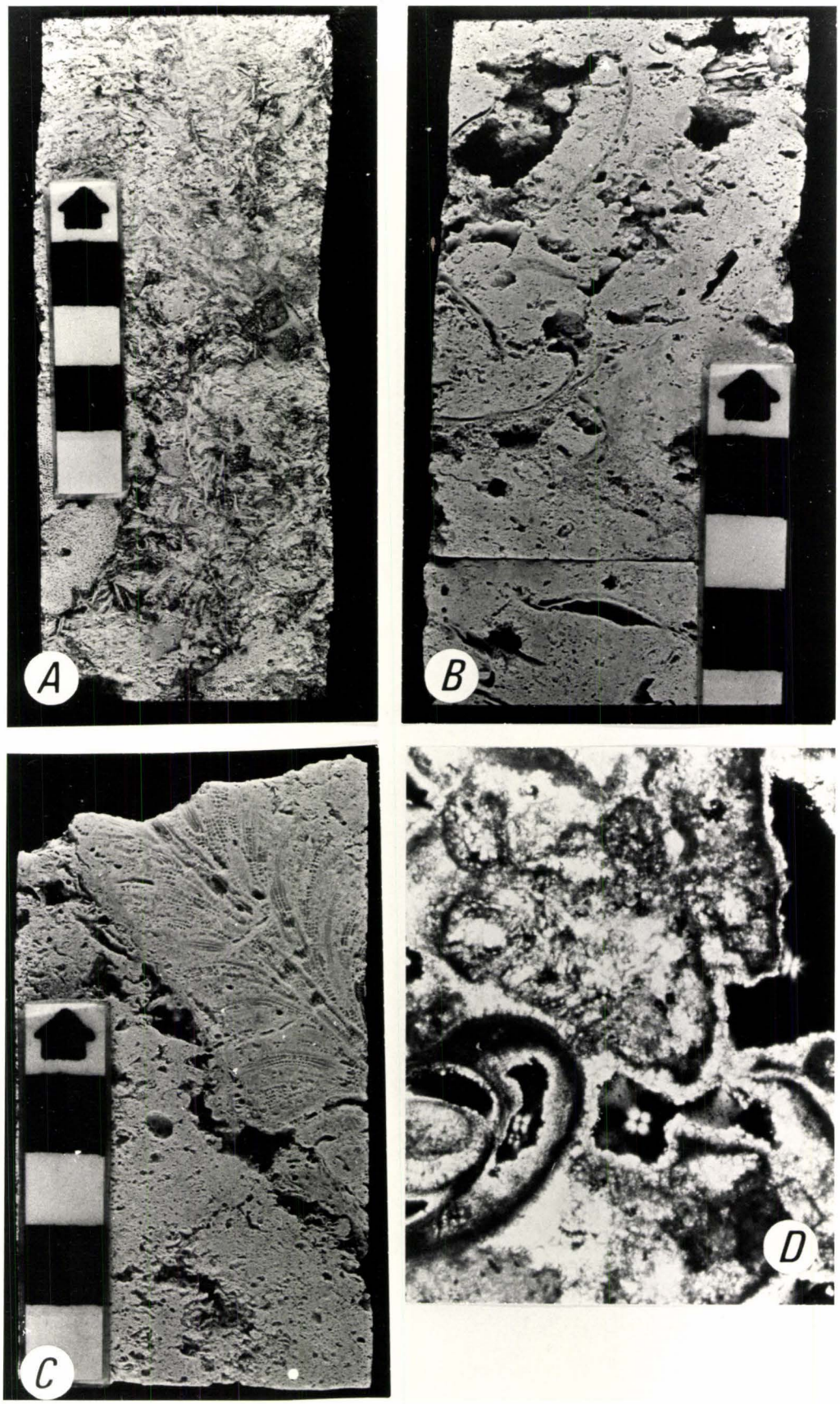
A
B
C
D

Halimeda is progressively leached at depth in Q5. At 2 m the plates are leached, distinguished by an elongate mold with micrite rimmed utricles which are sometimes spar filled, and enclosed in a micrite envelope of 10-40 µm thickness.

Coral fragments reflect a similar trend. Near the surface the corals appear recrystallized, are greyish with a grainy texture and often have a micrite envelope. Of all grains present corals appear to dissolve first, very near the top of the Q5 unit. The aragonitic composition of corals, like Halimeda, make them unstable in vadose conditions. Grains composed wholly of aragonite are being actively leached in Q5 resulting in common moldic porosity in the lower portion of Q5. X-ray diffraction analysis was conducted on one coral sample from Q5, RH-6 at 3.2 m from the surface, to determine if aragonite persists within unit Q5. This sample indicates complete alteration to calcite. In situ coral blocks are found in Q5, for a discussion of diagenesis within corals refer to Chapter 4.

Porcellaneous, benthic miliolid and peneroplid forams are common throughout Q5; Radial hyaline planktic forms are rare to occasional. The tests are medium brown in transmitted light with a Mg-calcite composition (Bathurst, 1976). Coralline algae also have a Mg-calcite composition.

Both forams and coralline algae are well preserved texturally.

Molluscs display much of the original texture and are rarely leached. This may be a function of mixed mineralogy, a combination of aragonite and calcite. The internal nacreous layer lining the inner shell may display partial dissolution because of its aragonitic composition.

Towards the base of Q5 original textures are progressively less well preserved. Micritic grains increase with depth becoming apparent at 2 m and common at 3 m.

II. Porosity

Q5 has four characteristic types of porosity based on Pray and Choquettes (1970) porosity classification; these are: primary intraskeletal porosity, solution enhanced interparticle porosity, moldic porosity and vuggy porosity. The first three porosity types are fabric selective, while vugs are non-fabric selective.

Primary porosity is syngenetic with the deposition of carbonate sediment, before the intervention of diagenesis. The internal chambers of forams and utricles of Halimeda are examples of such pores. The average primary porosity for Q5 is 0.87%. Intraskeletal porosity is most common in the upper 1.5 m of Q5, below this micrite cement and/or

calcite spar tend to fill the small intraskeletal cavities, reducing the porosity. The presence of primary porosity in Q5 is significant because it is generally absent in the older Q4B, Q4A units.

Interparticle porosity is primary, however the dissolution of grains protruding into interparticle pores indicates solution enhancement. For this study solution enhanced interparticle porosity was subjectively classified as secondary porosity by the author. In actual fact this porosity represents a transition from primary to secondary porosity. Q5 porosity is mainly of this type.

Moldic porosity develops when grains are leached leaving voids that retain the shape of the dissolved grain. Micrite envelopes, a concentration of micrite around the original grain (Coniglio, 1980) or early cements may serve to retain the original shape of the grain. Halimeda plates and coral fragments are most commonly leached, leaving voids. Moldic porosity increases from occasional in upper Q5 to common below 2.1 meters.

Vugs and macroscopic features are not easily studied using standard petrographic techniques, due to the small area of the average thin section. Vugs are unevenly distributed throughout the matrix and also a human bias exists in avoiding vugs when making thin sections. For

these reasons, point counting results do not coincide with a "zone of vugginess" observed for Q5 and Q4B, in core. Vugs 0.5-1 cm are occasional to common in the upper portions of Q5 from 0.30m-2.7m. A zone of larger vugs, 1-3 cm, exists from 2.1m-2.9m to the base of Q5, these vugs are abundant (PLATE XIII, Fig. B). From point counting results the average total porosity is 28.5%, and secondary porosity is 27.6%. From observation primary intraskeletal porosity and solution enhanced interparticle porosity are reduced to the base while moldic and vuggy porosity increase. The main type of porosity is solution enhanced interparticle porosity. There is no inverse relationship between grains and secondary porosity as in Q4B where moldic porosity is the main porosity type.

III. Cements

Cements are patchy throughout Q5. Areas with small grains in close proximity are better cemented. Patches of micrite appear to be poorly cemented, point counting results reveal an inverse relationship between spar and micrite but this may be a function of not seeing the cement associated with these microscopic grains. The variability of the cements must be stressed. The distribution of cement is highly variable, a multiple generation

cement with sparry calcite cement superimposed on micrite cement may exist in close proximity to pores devoid of cement. Slide 7, RH-2 shows evidence for preferential cement infill of smaller pores. Voids larger than $\frac{1}{4}$-$\frac{1}{2}$ mm are generally devoid of cement. Cements are located at grain contacts (PLATE III, Fig. C). Crystal terminations of calcite spar are commonly anhedral and blunted. Calcite spar accumulates on the underside of large or horizontally elongate grains (PLATE III). At these locations mosaic textures, (small equant crystals grading to coarse crystals away from the grain surface) may develop, often with euhedral crystal terminations. In the upper half of Q5 the cements are located in interparticle pore space and intraskeletal porosity (PLATE II, Fig. D). In the lower portion of Q5 where moldic porosity becomes common, cements may rim the interior of the molds. Occasionally molds are infilled with mosaic calcite spar.

In RH-2, slide 7 at 2.9 m some pores have 1 sheet of optically contiguous calcite cement. In RH-5, slide 6 at 2.4m shows syntaxial overgrowth of cements within a coral fragment such that calcite spar cement is in optical continuity with the recrystallized coral. Both of these observations are from locations in Q5 immediately above the Q4B surface. Ferroan calcite cement is absent

PLATE III Q5-VADOSE PENDANT CEMENTS

Fig. A: RH-2 slide #2 @ 2' (.61m)
Grains from a well cemented area in Q5. The two large grains have equant sparry calcite pendant cements (arrows) on their undersides due to gravity and large surface area for accumulation of percolating fluids.

Fig. B: RH-5 slide #4 @ 5' (1.5m)
Elongate Halimeda plate with a single generation of vadose calcite cement on the underside of the grain. Notice the irregular inner boundary of the micrite envelope indicative of algal boring. The utricles are rimmed in micrite and infilled with calcite spar, in part.

Fig. C: RH-5 #6 @8' (2.4m)
Calcite cement localized at grain contacts, resulting in pore rounding.

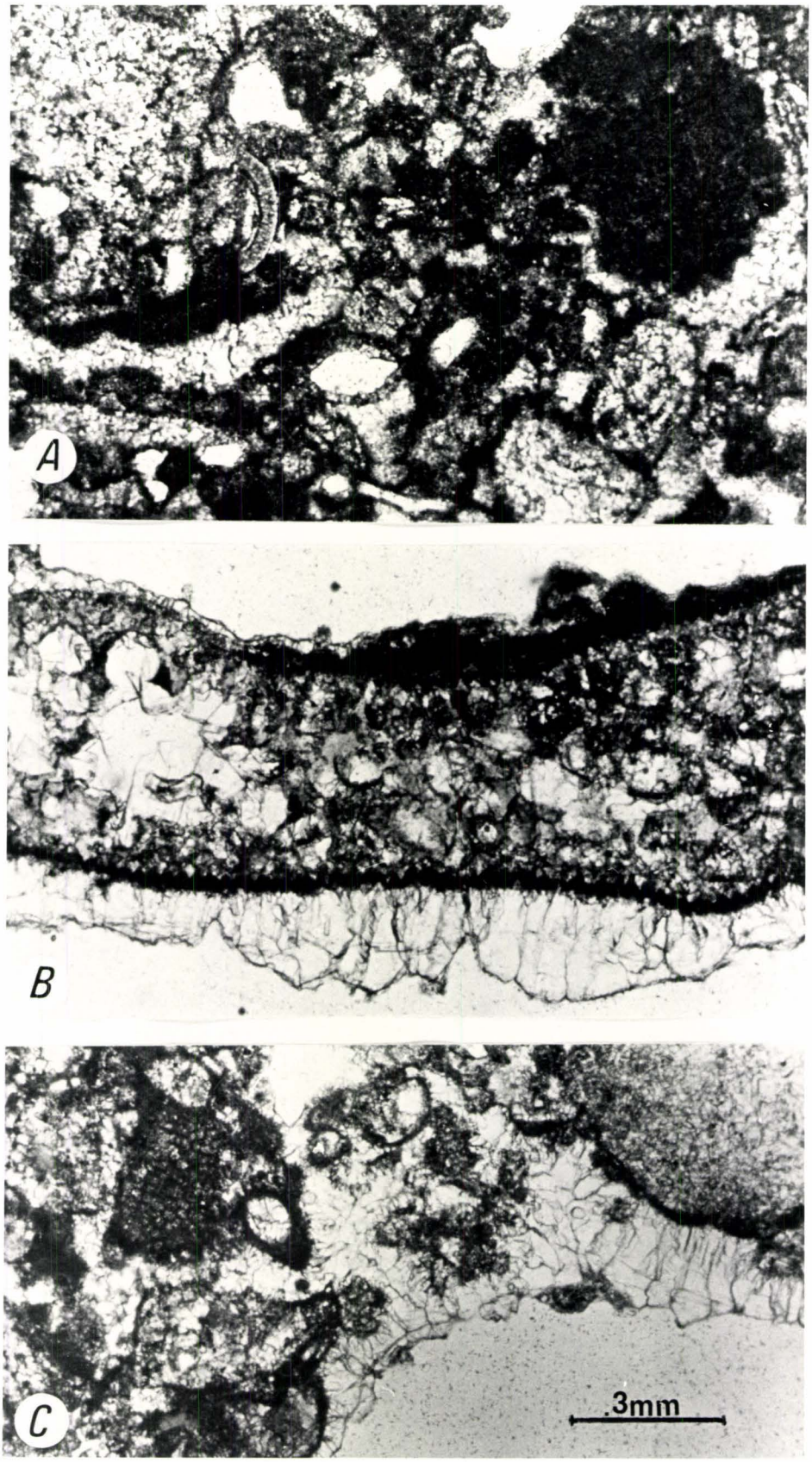
A
B
C
3mm

in Q5. The average value for total cement in Q5 is 27.8%, of this 21.1% is equant calcite spar, 2.84% micrite cement and 3.88% micrite envelopes.

Q5 Discussion and Interpretation

Surface seawater is usually supersaturated with respect to calcite. The presence of Mg^{2+} ions, however, in concentrations of greater than 0.05 mole/liter results in the inhibition of calcite precipitation in favour of aragonite and Mg-calcite precipitation (Berner 1971, in Friedman 1975). Marine cements are characteristically acicular aragonite and micritic Mg-calcite, although other morphologies are possible. Aragonite and Mg-calcite are stable in marine environments. In meteoric environments, vadose or phreatic, due to low concentrations of Mg^{2+} ions calcite is precipitated as the stable form, often as equant spar or bladed crystals. In a meteoric environment, slightly acid meteoric waters take aragonite into solution as follows: $CaCO_3$ (arag.) + H_2O + $CO_2 \rightleftharpoons Ca^{2+} + 2HCO_3^-$. The solution becomes supersaturated with respect to $CaCO_3$ and calcite precipitates (Friedman, 1975). Grains composed wholly of aragonite are being leached in Q5, resulting in common moldic porosity in the lower part of the unit. The leached aragonite, especially from Halimeda and corals in Q5 provided a source of dissolved $CaCO_3$. Areas near

leached coral fragments tend to be well cemented. As the solution becomes supersaturated with respect to $CaCO_3$, calcite cements precipitated within Q5. The source of cement in Q5 is predominantly autochthonous, with some allochthonous cement due to leaching at the surface.

Unlike aragonite, Mg-calcite tests; such as coralline algae, are not leached in Q5, instead the primary texture is retained. Magnesium may be leached from calcite very early in diagenesis, or paramorphic replacement involving micro-scale solution of Mg-calcite and precipitation of calcite may result in retention of the original texture (Friedman, 1964). In a meteoric vadose zone, this process may occur as rapidly as 7000-10,000 years (Gavish and Friedman 1969 in Friedman 1975).

X-ray diffraction of a Q5 coral sample indicated that the coral had completely altered to low magnesium calcite. Lowenstams' data for samples from the Upper Key Largo Limestone, synonymous with Q5, indicate the persistence of aragonite (Lowenstam 1954 in Stanley). Areas directly exposed to meteoric conditions, such as the portion of Q5 exposed along the Key Largo waterway (PLATE I), would be most susceptible to alteration while other less exposed areas might retain an aragonite composition (Stanley 1966). Perkins (1977) attributes the greater

percentage of aragonite in corals of Q5 relative to other units, as an indication that Q5 has been exposed to vadose conditions for a shorter period of time.

In the Upper Key Largo Limestone exposed along the Key Largo waterway Stanley observed that Halimeda was very abundant and extrapolated this to be characteristic of the Upper Key Largo Limestone. With better well control it becomes apparent that the abundance of Halimeda at this location is a local anomaly.

Solution enhanced interparticle porosity, classified as secondary porosity by the author, is the main type in Q5, setting Q5 apart from the other units. The moldic porosity of Q4B and Q4A is dependent on leached grains, and the interparticle porosity is plugged with calcite spar cement. This observation indicates that Q5 is diagenetically less mature than Q4B and Q4A.

Cements are precipitated from solutions supersaturated with respect to $CaCO_3$, loss of CO_2 may induce precipitation. In the present day Q5 vadose zone, rain water percolates down through the Q5 unit. The filling of a pore with cement requires evaporation or flushing through of many equivalent volumes of meteoric water (Longman, 1980). Q5 cements have a patchy distribution. Areas of fine grains in close proximity are better cemented than areas

of medium to coarse grain size. It is possible that fine grains have a greater surface area and a greater number of grain contacts which create capillary tension to hold films of water. At these sites precipitation of cements take place. Pore rounding is characteristic in Q5, where calcite precipitates at these grain contacts, rounding the residual pore space (Dunham, 1971). The pore spaces in the vadose zone have two immiscible phases - air and water. Crystals may exhibit blunted terminations when they become undernourished near the water-air interface. " .... the advance will decrease the space available for side-ways diffusion of ions to the tip of the growing crystal." (Dunham, 1971 p. 298). The starved crystal terminations are called meniscus cements. These meniscus cements are most common on the tops and sides of grains in Q5 where water films are thinnest.

Gravity cements (Muller, 1971) are very common in Q5, where droplets of water preferentially accumulate on the undersides of grains. Elongate, horizontal grains such as mollusc fragments or Halimeda plates are most effective (PLATE III). Where pendant or gravity cements grow into vacant cavities they often have euhedral crystal terminations. Many small crystals nucleate on the underside of the grain, the crystals oriented most

favorably elimate others in a competition for nourishment. The resultant texture is a progressive increase in crystal size away from the grain surface (Bathurst, 1969). Molds often are filled with such a mosaic of calcite spar; however this is uncommon in Q5 where most molds remain empty.

In RH-2 at 2.9 m optically continuous spar cement fills voids, and in RH-5 at 2.4 m within a coral, coral-lites are cemented with syntaxial overgrowths of spar cement, both of these cements indicate phreatic conditions. Both locations are directly above the Q4B discontinuity surface. Due to subaerial diagenesis discontinuity surfaces are better cemented. It is possible that meteoric water temporarily ponds on this, resulting in a perch lens.

Unit Q5 was deposited during an interglacial period approximately 125,000 years ago when sea level was higher than present day. Figure 3 shows eustatic sea level changes over the past 130,000 years based on Barbados data (Steinen et al., 1973). From this data it appears that Q5 has not been submerged since its deposition. The clarity of single generation vadose cements in Q5 suggests that no overprinting of other diagenetic environments has occured.

Within Q5 intraskeletal porosity tends to be the

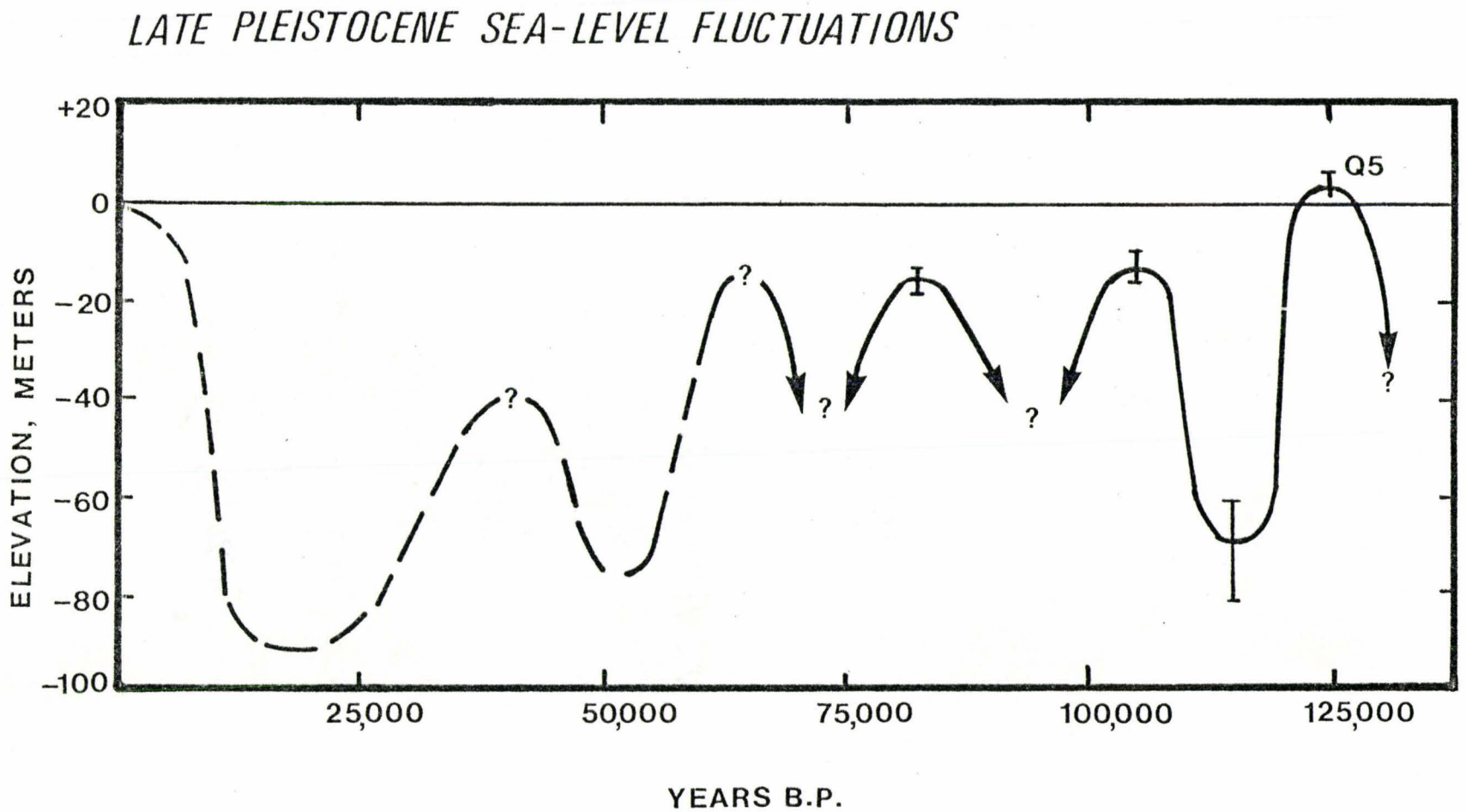

Figure 3. (modified from Steinen et al., 1973)

first infilled with generations of cement, this also occurs in Q4B, therefore this process will be discussed collectively for Q5 and Q4B. At 0.61 m in RH-2, Halimeda utricles are lined with micrite and less commonly filled with sparry calcite. The micrite envelopes around the periphery of the grain are believed to originate in the marine environment by the precipitation of micrite in vacated microscopic boreholes of algae (Bathurst, 1976). Utricles rimmed in micrite may be formed similarly by endolithic algae. The subsequent filling of utricles and foram chambers by calcite spar is an inorganic process. Friedman (1964) observed that the first stage of cementation is the reduction of intraskeletal porosity by early cements. Within Q5 the filling-in process is common below 1.2 meters. Are these cements of submarine or vadose origin? If these are submarine cements the absence of infilled chambers in the upper portion of the unit may be explained by the dissolution of marine aragonite and Mg-calcite cements by percolating meteoric water. Significant reduction of primary porosity may occur at the depositional interface (Glover and Pray, 1971). The composition of the cement often reflects that of the host, and crystals are oriented perpendicular to the host wall. "It seems likely that the cement has formed by directional

overgrowth of the more favorably oriented crystals of the skeletal host...." (Glover and Pray, 1971, p. 80). In Q4B, two generations of cements occur in forams, stubby equant calcite crystals oriented perpendicular to the test wall and subsequently the chamber is filled in with a mosaic of calcite spar. Moberly (1973) found that inorganic precipitation of Mg-calcite in intraskeletal pores takes 3 years, while aragonite takes more than 8 years. These cements were found at the deposition interface in closed well preserved chambers, not unlike the cements found in Q5 and Q4B.

4. UNIT Q4B

Observations

I. Grains

Q4B is characterized by very fine grain to medium grain wackestone to packstone, the most common constituent being very fine grain carbonate sand to mud (PLATE IV, Fig. A, C). Point counting reveals 23.5% grains and 22.17. matrix. Larger coral rubble and *in situ* coral heads float in a fine grain matrix. The fine grain material has similar grain constituents as Q5: Molluscs, *Halimeda*, corals, forams, and coralline algae. Rounded pelloids (0.5mm diameter) of dark brown micritic material with internal bioclasts are common throughout Q4B (PLATE IV, Fig. B). These pelloids are distinctly different from micritic grains, and are likely fecal in origin. The pelloids commonly occur in groups. In core, burrow mottling is common.

Micritic grains are common, increasing to the base of Q4B. In RH-2 at 5.9 m and RH-5 at 5.5 m and 6.7 m some grains are indistinct, with a loss of primary texture and blurred edges. Where individual grains are large enough to observe primary textures they seem to be highly altered, more so than in unit Q5.

Halimeda plates are recognized solely by micrite

PLATE IV Q4B

Fig. A: RH-2 @ 18.5' (5.64m)
This section of core is characteristic of the well cemented carbonate muds interspersed with in situ corals in Q4B. Note the burrow mottling and the small trains of bubbles at a 45° angle associated with dewatering processes.

Fig. B: RH-2, slide #11 @ 19.5' (5.94m)
Fine grain carbonate mud, indicative of that observed in core in Fig. A. The pelloid believed to be fecal in origin, is 0.5mm, dark brown micrite with incorporated bioclasts.

Fig. C: RH-2, slide #15 @ 27' (8.23m)
This thin section reveals the "classic" Q4B fine grain carbonate sand. Micrite envelopes surround molds of dissolved grains. Equant calcite mosaic fills many of these voids, completing the dissolution-precipitation process.


A

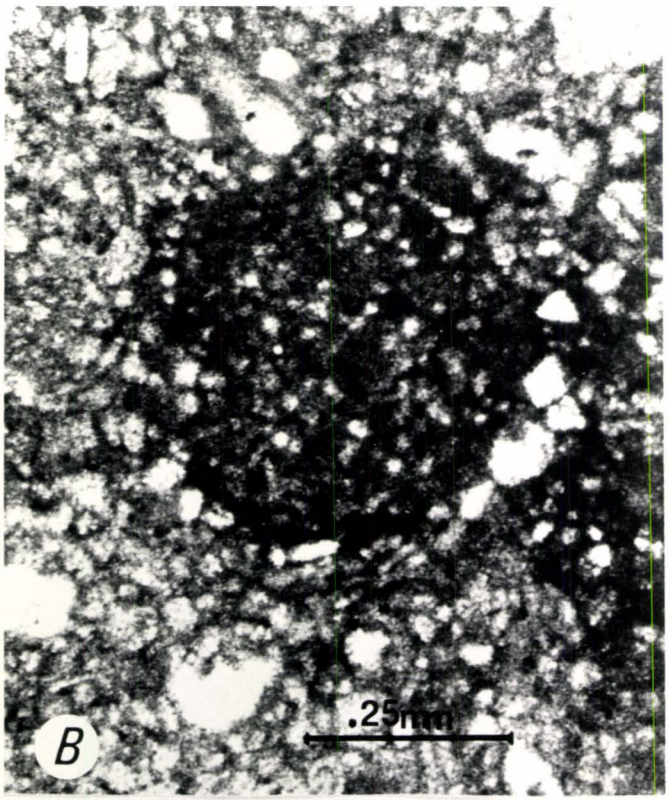
.25mm
B

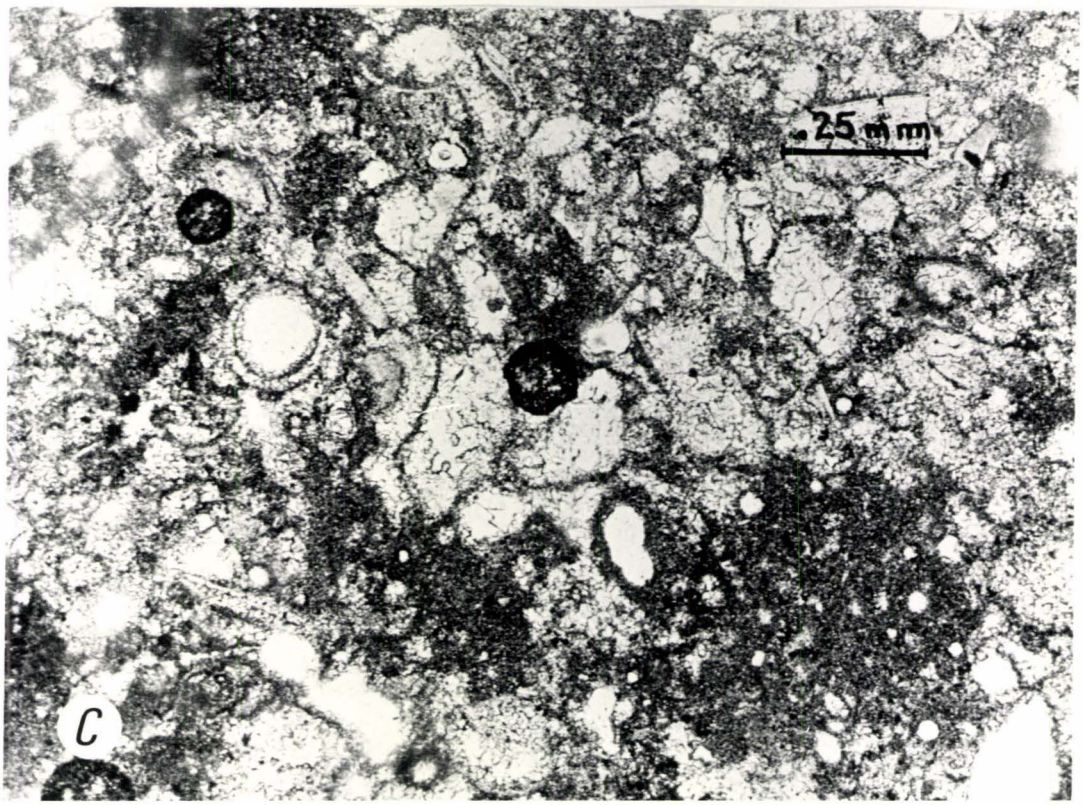
.25 mm
C

envelopes and utricles lined with micrite and filled in by calcite spar. Molluscs are partially to completely dissolved contributing to moldic porosity. Corals, the largest grain constituent, are recrystallized, often retaining a grainy remnant texture. Preservation may be a function of grain size. Larger mollusc fragments as in RH-2 at 5.9 m, have retained primary textures to a greater degree than smaller grains, as have larger corals and coral heads, where aragonite sheaves are still visible. Coralline algae, texturally well preserved in Q5 are leached at depths of 5.5 m-6.7 m in RH-5, Q4B. Rare quartz grains appear throughout Q4B becoming occasional to common near the base. These grains have irregular micritic embayments at their peripheries.

II. Porosity

Within Q4B there are two main types of secondary porosity: moldic and irregular vuggy porosity. Intergranular porosity and primary intraskeletal porosity are plugged with equant calcite spar.

Point counting results indicate an inverse relationship between grains and secondary porosity reflecting the dependence of moldic porosity on grains. The average porosity for Q4B is 28.5%, of which 27.9% is secondary porosity. In micrite rich areas, molds and vugs surrounded by micrite are not reduced by calcite spar.

In RH-5 at 6.7m-7.6 m, irregular dissolution vugs (.75 x 1cm) are more abundant than moldic porosity. These vugs may be due to: solution enhanced interparticle porosity, solution enhanced and coalescing moldic porosity or irregular non-fabric selective dissolution. There is very little cement in these vugs.

Commonly vuggy porosity has dimensions 2mm by 20mm and larger. A zone of macroscopic vugginess can be defined for each core, the upper limit is: RH-2 8.2m, RH-5 5.5m, RH-7 4.0m and RH-6 3.0 m from the present day surface. These are 3.3m, 2.7m, 2.4 and 3.1m respectively, from the Q4B sub-aerial surface. This is similar to Q5 where 2.1-2.9m marks the upper limit of the vuggy zone. Vug walls are solution enhanced, they follow grains in an irregular fashion, along the path of least resistance. Vugs are most often devoid of cement except in a few locations which will be discussed in Chapter 6. In core, the vuggy porosity has an elongate channel-like appearance similar to the morphology of a burrow.

The morphology of grains effects diagenetic processes to a noticeable extent. Around the periphery of larger grains, such as molluscs and corals heads, are porous zones (PLATE II, Fig. B,C). These zones are produced by settling of the matrix away from the grain surface during compaction. The large grain provides a path of directed flow for percolating fluids around the periphery of the grain resulting in dissolution.

III. Cements

The total average cement content for Q4B is 27.9%. This can be subdivided into calcite spar 22.7%, micrite cement 2.1%, and micrite envelopes 3.3%. (Appendix A).

No ferroan calcite cements were found in Q4B. Intergranular porosity is plugged with equant calcite spar. Where crystal terminations exist they are most often blunted. Pendant cements are rare to occasional, exhibiting two generations of calcite spar. Most grains are too small to observe the cement morphology, but where this is possible cements seem to be thickest at grain contacts. Intraskeletal porosity is infilled with two generations of cements, as previously described. Fibrous acicular cement is present in some inner chambers of forams. Rare examples of acicular cement, adjacent to grains, and encased in calcite spar are found at RH-5, 7.6m and RH-2, 3.4 m. Molds retained by micrite envelopes are infilled with calcite spar mosaic. At certain intervals within 4B euhedral blades of calcite cement in a radiating botryoidal manner are associated with the secondary vugs and channel porosity. A detailed discussion of these observations is given in Chapter 6.

Cementation within Q4B Corals

Cements within corals are more variable than in the matrix. The corals are coarsely recrystallized, often retaining a dark grainy remnant texture, and less commonly

the original aragonite bundle texture. Marine sediment, a dark brown, micrite with internal bioclasts, has been flushed into the corallites, especially at the periphery of the coral head. This may form geopetals within individual corallites, settling at the lowest portion of the corallite due to gravity. "Way up" indicators are useful to determine the orientation of the coral when the sediment was flushed in. If the coral has remained in situ these geopetals are true way-up indicators (PLATE V, Fig. B).

Acicular cements, 5 μm by 50 μm, line intraskeletal voids, preserved where encased in clear calcite spar. This was found at RH-5, 4.6 m and 7.2 meters (PLATE V, Fig. C). The acicular cement in part, has suffered a partial loss of individual crystal identity becoming a brown micritic rim with relict fibrous textures. Syntaxial plates of spar in optical continuity with the recrystallized coral encase the acicular cement. The aragonite needles are frequently dissolved where they make contact with the grain. There is no calcite at this point encasing and protecting the aragonite from dissolution. Some corallites have 10-30 μm micrite rims due to the boring activity of endolithic algae. The corals are extensively bored with straight tubules having a 1-2 μm diameter.

Four generations of cement are found in Q4B corals. In order from oldest to youngest, these are: 1. a thin rim

PLATE V CEMENTS IN CORALS

Fig. A: RH-2, slide #13 @ 21.5' (6.55m) Q4B
Dark micrite rim, due to boring activities of endolithic algae immediately adjacent to the corallite wall. Calcite spar with anhedral terminations overlies the micrite. The voids remain open except where lime mud, with a dark pelleted appearance, has been flushed in. The dark grainy texture is due to organic residue.

Fig. B: RH-5 slide #13 @ 19.5' (5.94m) Q4B
Large crystal size in coral due to aragonite-to-calcite inversion. Lime mud geopetal. Cross-polars.

Fig. C: RH-5, slide #6 @ 8' (2.44m) Q5
Marine acicular aragonite needles 50 µm long, preserved and encased in vadose calcite spar cement.

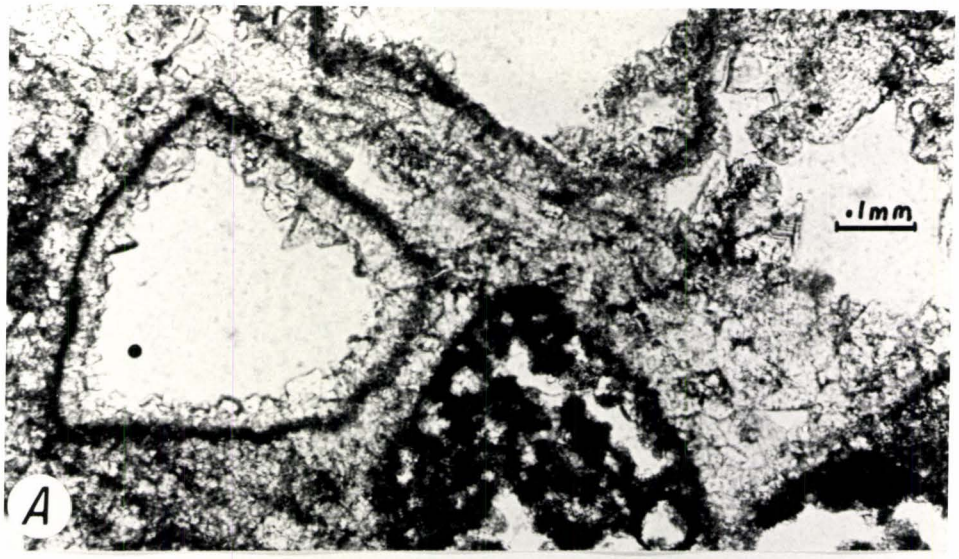
.1mm
A

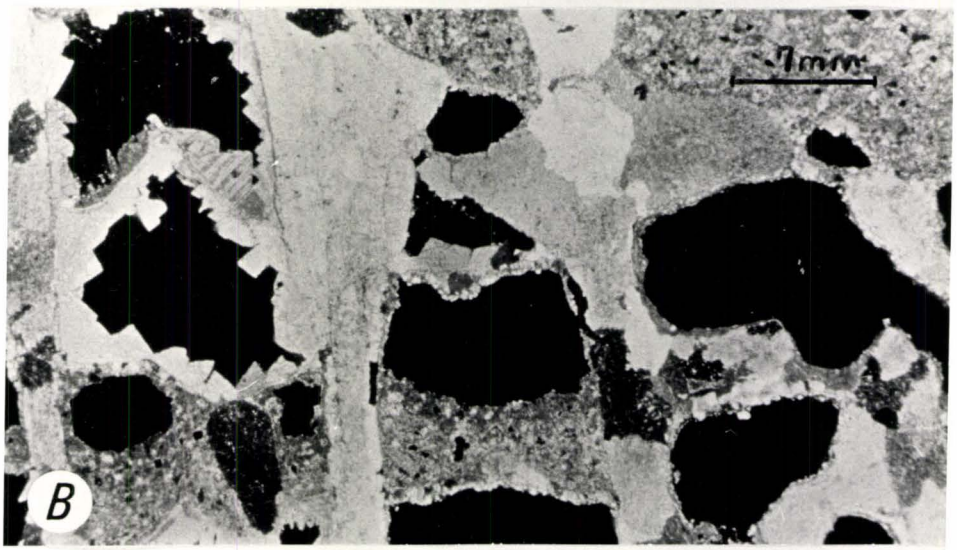
.1mm
B


C

of micrite cement, 2. equant crystals of calcite spar, 3. micrite and 4. a thin rim of calcite spar. One or all four cements may be present. Generally intraskeletal porosity is not completely filled. Calcite spar crystal terminations may be euhedral, blunted starved crystals or corroded crystals showing evidence of dissolution.

At RH-5 5.8 m, acicular cement replaces generations 1 and 3 listed above. The acicular cement is encased and preserved in the overlying calcite spar. Sometimes the acicular cements align with the original acicular bundle texture of the corals. Calcite spar may form optically continuous plates with the recrystallized coral. The cements are conspicuously clear, while the coral has a darkened grainy texture.

Q4B Discussion and Interpretations

Q4B was deposited during a high stand of sea level at 180,000 years B.P. The topographic relief of the unit established the orientation of the linear arcuate Keys as they appear today (Perkins 1977, pg.176). Q5 was subsequently deposited on this topographic high at 125,000 yrs B.P. when sea level inundated the Q4B surface.

Dissolution-precipitation processes have eliminated the primary textures of the grains to a much greater extent than in Q5. Interparticle porosity is plugged with equant calcite spar cement. Point counting reveals the

inverse relationship between grains and secondary porosity. This is because secondary porosity is almost exclusively moldic, which is dependent on the dissolution of grains. The average porosity of Q4B is 28.5% the same as that for Q5. Although porosity values are similar, actual porosity types are not. Q5 has solution enhanced interparticle porosity, which is modified syngenetic primary porosity. In Q4B, moldic porosity is indicative of the progressive stabilization of minerals from the meta stable minerals, aragonite and Mg-calcite. Q4B is diagenetically more mature than Q5.

A vuggy zone with an upper limit 2.3 m-3.3 m from the Q4B subaerial surface is comparable to a similar zone at 2.1 m to 2.9 m from the Q5 surface. This vuggy zone extends to the base of the unit. The vug walls are solution enhanced, following grains in a random way that suggest non-fabric selective processes. Throughout Q4B, burrow mottling (PLATE IV, Fig. A) and the presence of fecal pellets (PLATE IV, Fig. B) provides evidence for burrowers. Vugs and channel porosity may be partially controlled by solution enhanced burrows. The observed zonation of the vugs is more difficult to explain. Perhaps at the range of 2.1 m to 3 m from the surface, meteoric waters percolating down through the vadose zone are channeled along paths of directed flow. Interparticle porosity may have been

cemented by slower moving solutions that had sufficient exposure to overlying carbonates to become supersaturated with respect to calcite. As a result leaching solutions were directed repeatedly to better drained areas enhancing and enlarging vug and channel porosity (Dunham, 1971).

Q4B was deposited 180,000 years B.P.. At 125,000 , Q5 was deposited, and Q4B was once again inundated. The knowledge of sea level fluctuations between these dates is unclear. In Q4B packstones there is subtle evidence for 2-generation vadose pendant cements. Within coral heads, acicular marine cement is encased in vadose spar; this pattern repeats twice. Both multiple generation cements imply two cycles of marine to vadose conditions. The Q4B carbonates were exposed to vadose conditions for an unknown period of time between the depositon of this unit at 180,000 yrs B.P. and the marine transgression responsible for the depositon of Q5 at 125,000 yrs B.P. (Fig. 3). After the deposition of Q5 sea level dropped exposing Q4B overlain by Q5, to vadose conditions for almost 125,000 years. The dissolution of $CaCO_3$ in Q5 supplied an allochthonous source of calcite cement to Q4B, This explains the plugging of interparticle porosity in Q4B. Point counting results do not indicate an increase in cementation in Q4B.

Reduction of intraskeletal porosity of corals is

an early diagenetic process occuring in the submarine environment. Micrite envelopes with irregular inner boundaries indicate the activities of endolithic algae (PLATE V, Fig. A). Marine lime mud with bioclasts was flushed into the corallites (PLATE V, Fig. B) and acicular needle-like cements (50 μm length) rim the corallites reducing primary porosity (PLATE V, Fig. C). Pingitore (1976) acknowledges the later two marine fillings as having quantitative importance. The aragonite needles are preserved where encased in blocky calcite cement of probable vadose origin. Similar textures have been observed by Pittman (1974) and Pingitore (1976). The aragonite mineralogy of the needles has undergone "inversion" to calcite, a process of solid state stabilization whereby original texture is retained (Land, 1967). The coral skeleton has recrystallized in a similar manner. The dark grainy appearance gives the impression of preservation of fine textural detail. This darkened material is organic tissue, most commonly found in vadose altered corals (Pingitore 1976, p. 993). Intraskeletal porosity in Q4B corals is not completely filled with cements; this too is indicative of vadose cementation. Alteration and cementation patterns in Q4B corals suggest the main diagenetic environments have been vadose.

5. UNIT Q4A

Observations

The Q4B/Q4A break is subtly defined by random pockets of reddish brown micrite and a lithologic change to a quartz bearing light grey carbonate (PLATE VI). The quartz bearing unit occurs at a fairly constant horizon at: RH-2 9.1 m, RH-5 8.7 m, RH-6 9.3 m, and RH-7 at 7 meters from the present day surface. The thickness of the unit varies from 1.8 m at RH-2 to 1.1 m at RH-5.

I. Grains

This unit is a medium to coarse grained packstone to grainstone. A wackestone is associated locally with sub-aerial diagenesis at the Q4A/Q4B break. Quartz grains and mollusc fragments dominate with minor forams and corals. Point counting results range from 15.9-39% grains with an average of 26.4% grains for Q4A. The matrix constitutes 19.1% of Q4A. The common to abundant quartz is medium to coarse grain, .25-.75 mm, generally subrounded and well sorted (PLATE VI, Fig. C). RH-7 located away from the seaward face of the Key has less quartz and a smaller grain siz. Sub-parallel dustlines or lines of inclusions due to healed fractures, may tranverse the grains (PLATE X). These inclusions are lines of weakness in the grain. Throughout

PLATE VI Q4A

Fig. A: RH-2, Q4A
Abundant moldic porosity due to the dissolution of aligned mollusc fragments. Notice the 15-17° angle lamination. The unit is well cemented.

Fig. B: RH-5 @ 32' (9.75m)
Immediately overlying the Q3 laminated exposure surface (in the lower left corner) is a 6cm horizon of angular rip-up clasts. This is a transgressive lag deposit.

Fig. C: RH-5 slide #20, @ 29.5' (8.99m)
Well sorted subrounded quartz grains and recrystallized mollusc fragments with equant calcite spar plugging interparticle porosity Cross polars.

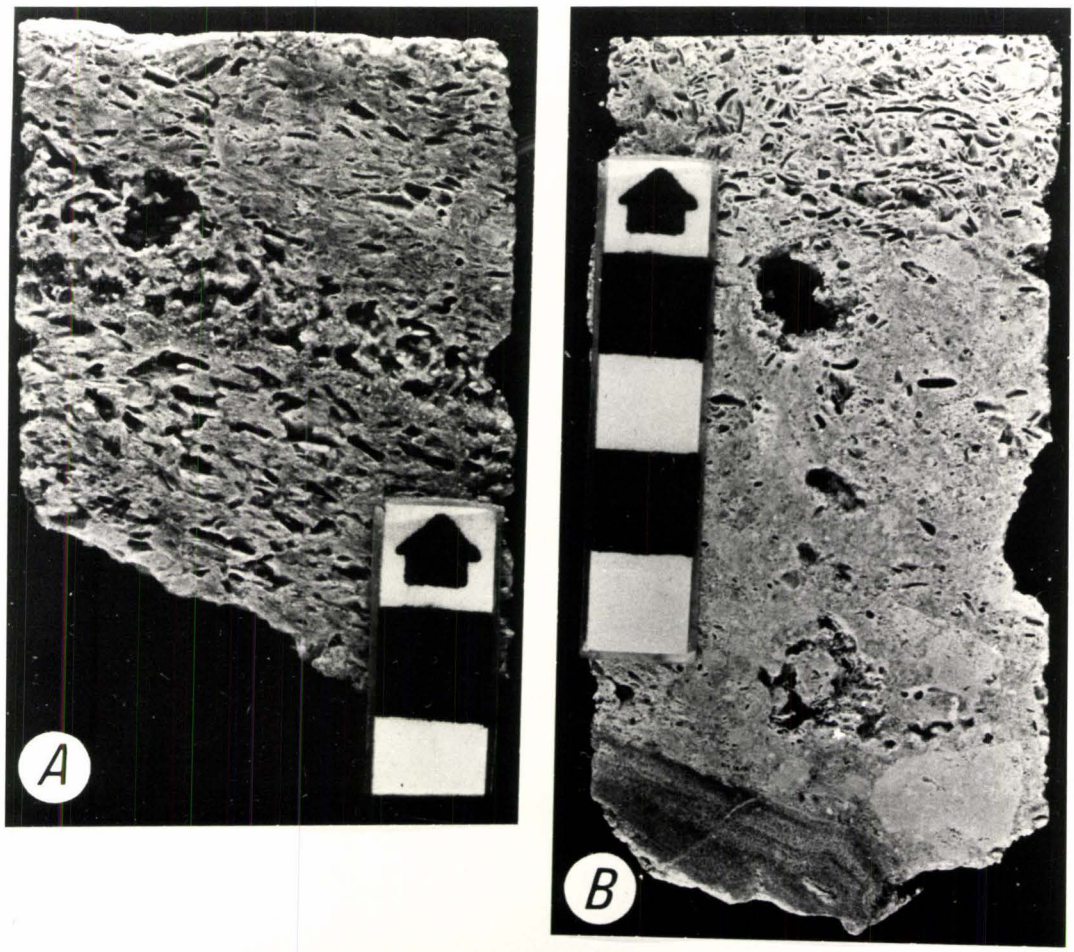
A
B

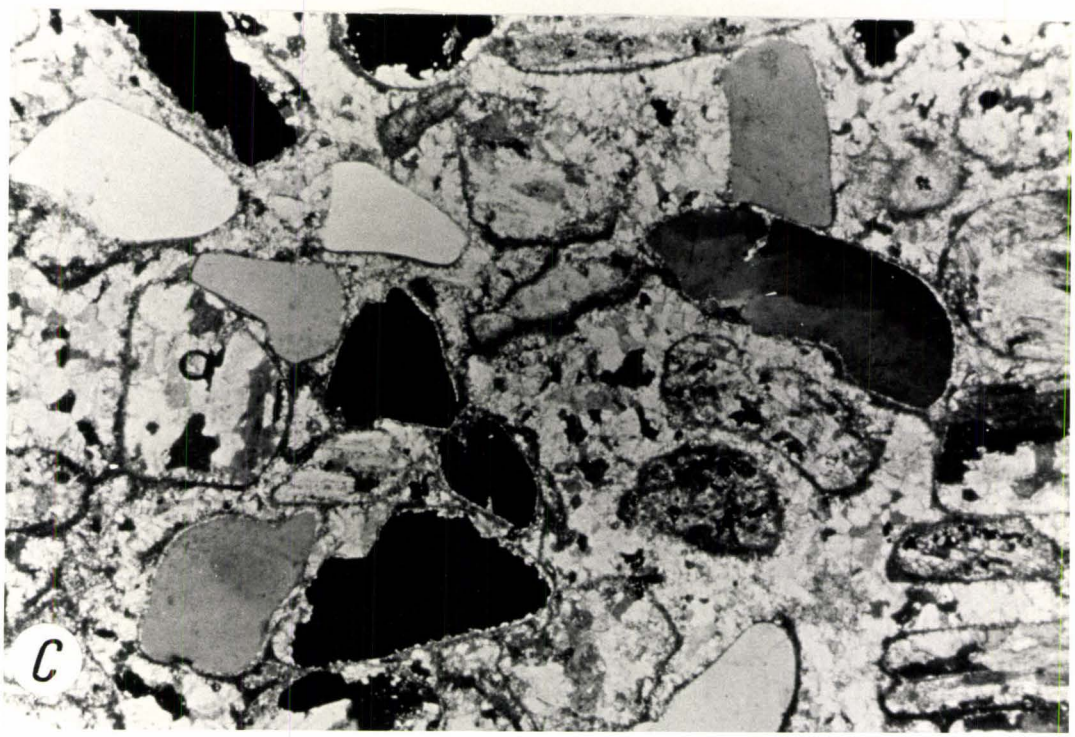
α
C

Q4A, evidence for dissolution of quartz is common and varied. Quartz grains commonly have irregular edges and micrite embayments (PLATE X, Fig. C). Preferential dissolution occurs along lines of inclusions with subsequent precipitation of micrite (PLATE X, Fig. C). Partially dissolved quartz grains remain in molds, leaving evidence that the entire mold was originally occupied by the quartz grain. In RH-2 at 9.6 m molds resemble the size and shape of quartz grains, in contrast to molds that resemble mollusc fragments.

Roughly 25% of the quartz grains in Q4A have 2-3 boring-like penetrations, filled with micrite that extend into the grain from the grain surface in a perpendicular to sub-perpendicular orientation (PLATE VIII). The walls are unlined and parallel, having a diameter of 3-12 μm's, most commonly 10 μm's. These structures may bifurcate or curve. Where boring-like structures are found dustlines are often absent.

Two quartz samples from Q4A: RH-2 9.6 m and RH-6 9.5 m were dissolved from the carbonate matrix using a 10% HCl solution. The 3-D quartz grains were mounted on SEM stubs, observed and photographed. The quartz surfaces revealed dissolution features such as crescentic impact features enhanced by dissolution (PLATE IX).

The boring-like structures, 2-12 μm diameter,

have entrances at the grain surface that appear to be solution enhanced, this leads quickly to the slightly recessed cylindrical morphology of the borehole (PLATE IX).

Staining for ferroan cements revealed the presence of an amorphous iron compound, associated with the quartz grains. The iron compound assumed a brilliant cobalt blue coloration due to the reaction with the potassium ferrocyanide in the stain. Closer observation revealed occasional flecks of a yellowish metallic mineral embedded in the quartz, possibly pyrite, although no euhedral cubic crystals were found in these samples. A sample from Q4A, RH-5 showed banding of quartz containing the iron compound to that without, possibly segregation due to settling processes.

Mollusc fragments in Q4A are generally recrystallized, with better preservation of primary texture than molluscs in the younger Q4B unit. Individual borings are occasional to common around the grain periphery, micrite envelopes are common. The elongate mollusc fragments are of constant size up to 4 mm, well sorted, often larger than the associated quartz grains, and may be aligned parallel to sub-parallel. In core, RH-5, RH-2 and RH-6 display a well sorted, banded appearance due to the sub-parallel orientation of the mollusc fragments. The banded appearance in RH-2 is further enhanced by a light to medium grey color variation (PLATE VI, Fig. A). Low angle bedding,

15-17° is distinct at RH-2, and vaguely suggested at other locations. At the base of Q4A overlying the Q4A/Q3 contact in RH-5 there is a 6 cm zone of jagged rip up clasts, 1-2 cm in diameter (PLATE VI, Fig. B), and in RH-6 a horizon of very coarse mollusc debris. These are probably transgressive lag deposits.

II. Porosity

Within Q4A porosity varies over small vertical distances. Porosity ranges 7.9-50.5% with an average porosity of 29.3%. Moldic porosity is common to abundant, a major proportion being leached mollusc fragments. A minor amount of moldic porosity resembles quartz grains. Interparticle porosity is often plugged, intraskeletal porosity is absent. Occasionally 2-3 mollusc molds coalesce resulting in larger pores. In RH-2 at 9.1 meters, irregular dissolution vugs are present; at 9.6 m vugs 2-10 mm, are common. The control appears to be non-fabric selective.

III. Cements

The Q4A unit is generally well lithified with intergranular porosity plugged by equant calcite spar. Ferroan calcite cement is absent. The cements of this unit have four generations, from oldest to youngest, these are: 1. a 20 μm dark brown micrite, 2. a 100 μm rim of calcite spar or acicular cement, 3. a micrite rim, 15-20 μm thick and 4. an equant calcite spar mosaic of irregular thickness

PLATE VII Q4A CEMENTS

Fig. A: RH-2, slide #17 @ 30' (9.14m)
Recrystallized mollusc fragments with preservation of original fabric. Two generations of cements are present: 1) Micrite (arrow); 2) even rim of elongate calcite spar, probably an alteration of acicular aragonite cement. These 2 cements have been interpreted as altered beachrock cement.

Fig. B: RH-2, slide #17 @ 30' (9.14m)
Grains rimmed with 50 μm wide band of remnant acicular cement encased in calcite spar. The void infilled with equant calcite spar of vadose origin.


A

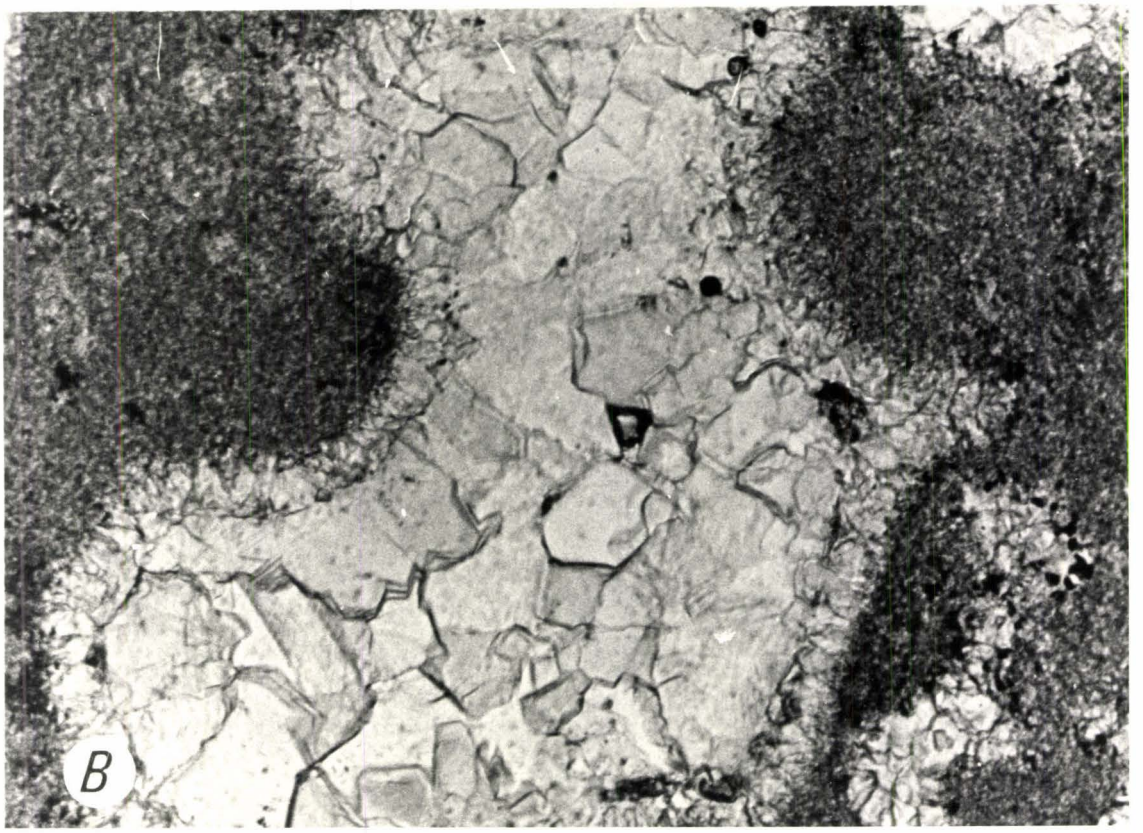
B

PLATE VIII BORINGS IN QUARTZ GRAINS, Q4A

Collectively Fig. A, Fig. B, Fig. C; RH-2, slide #17 @ 30' (9.14m)

These parallel walled embayments intruding from the periphery of the grain may be vacated micrite filled boreholes with a 3-12μm diameter. Notice Fig. B, the preposed borehole bifurcates and Fig. C, the borehole is slightly arcuate. These morphologies should be compared to the straight embayments of micrite that have formed inorganically by preferential dissolution at high pH's of dustlines and inclusions in the quartz grains (PLATE IX). These quartz grains do not show dustlines.

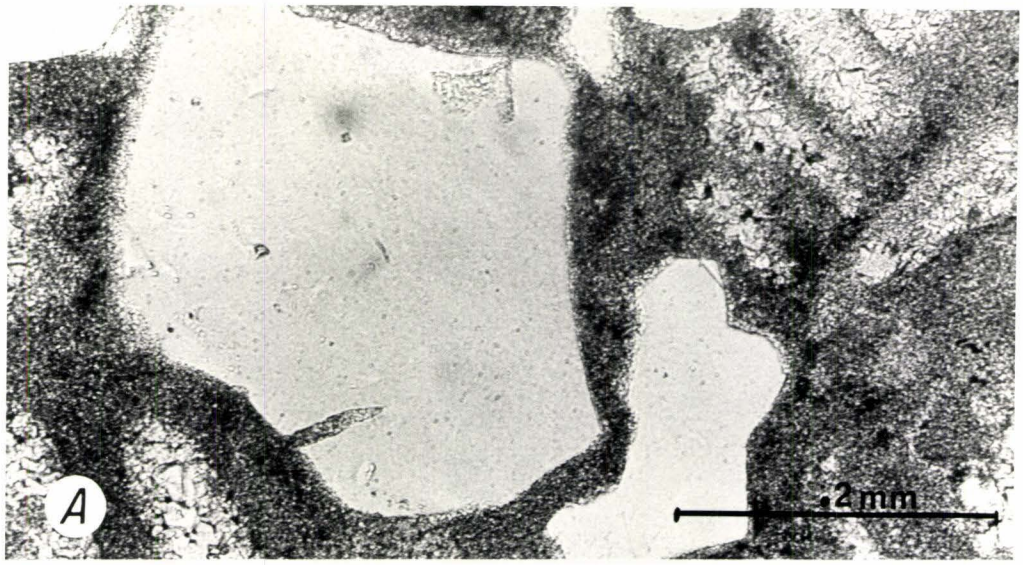
A
.2mm


B

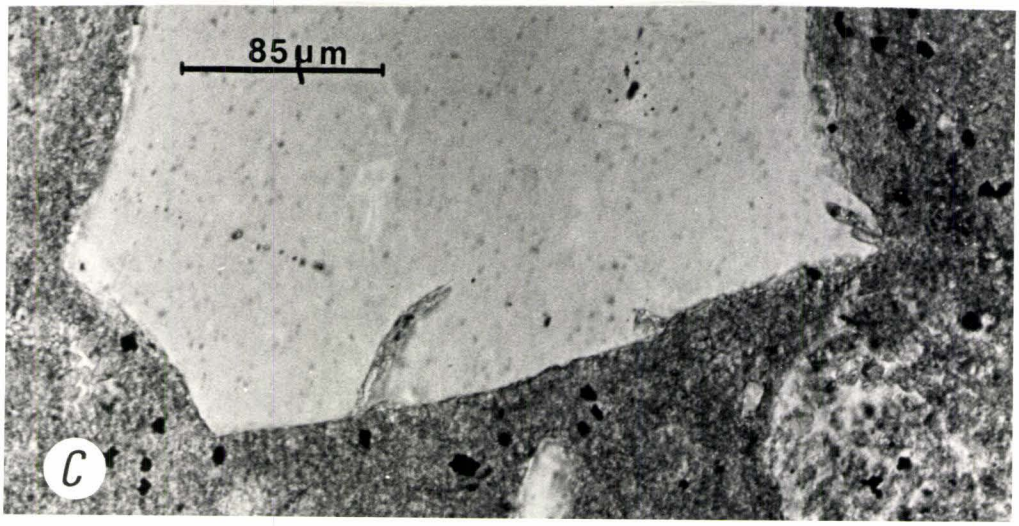
85µm
C

that often fills the pore.

The micrite cement has a sharp contact with the grain and is fairly evenly distributed about the entire grain. The micrite is sometimes thickest on the tops of large grains, as though flushed in from above (PLATE VII, Fig. A). For point counting this micrite was classified as micrite cement. Often this overlies and obscures micrite envelopes whose inner margins are irregular showing evidence of boring. Q4A has 3.5% micrite, this is more than that for Q4B or Q5. The second generation cement is a clear rim of calcite that has one of two possible morphologies: 1. elongate crystals (100 μm), oriented perpendicular to the grain surface as seen in RH-2 at 10.4 meters and 2. relict textures of acicular cement encased in calcite spar as seen in RH-2 between 9.1 meters and 10.4 meters (PLATE VII, Fig. B).

The third generation micrite may or may not be present, while the fourth generation equant calcite spar is present. In places this spar is partially leached.

Throughout Q4A there is a vague suggestion of pendant cements, especially in relation to the second generation rim of calcite spar that is best developed on the top and bottoms of grains.

Q4A Discussion and Interpretations

Wells RH-2, RH-5 and RH-6, from north to south on

the eastern coastline of Key Largo, reveal a trend in reduction of quartz to the south. This indicates a clastic source to the north. RH-7, on the western shoreline of Key Largo, has less quartz and a smaller mean grain size. The paleotopography during Pleistocene times was such that to the north the Brighton High and the Immokalee High supplied clastic debris to the Allapatah lobe a spit-like extension of the Brighton High (Perkins, 1977), (Fig. 5). The Q4A quartz is likely reworked Allapatah Lobe quartz, carried via longshore drift by the counter current which flows along the eastern Florida shoreline to the south. The position of RH-7 on the western margin removed it from the direct effect of longshore drift, reducing the clastic quartz input. The subrounded quartz grains indicate considerable transport and/or reworking. The present day Key Largo coastline is not made up of quartz sand. Biscayne Bay to the north acts as a sink for clastic quartz (Harrison, person. commun.). During Q3 and Q4B carbonate deposition, a similar sink may have existed to the north to explain the absence of quartz. Q4A represents a point in time when clastic quartz was not trapped to the north. A raise in sea level might explain the inefficiency of a paleotopographic trap. Q4A grains are well sorted quartz and molluscan debris. The elongate mollusc grains are generally larger than the subrounded quartz grains, perhaps a function of

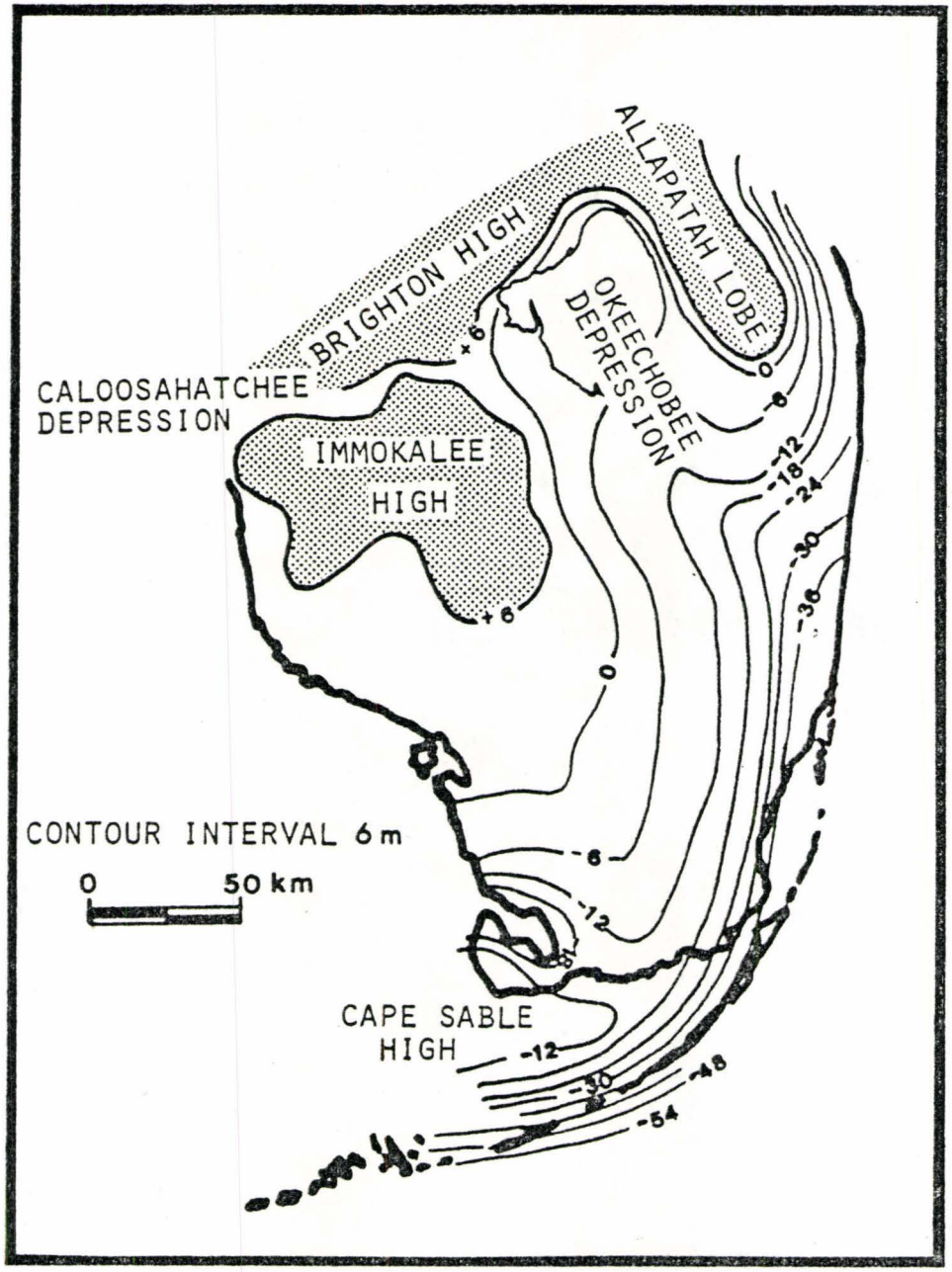

Figure 4. Pre-Pleistocene paleotopographic features of South Florida. Contours related to mean sea level. (modified from Perkins, 1977 in Coniglio, 1980)

sorting via settling velocities. The large flat surface of a mollusc grain offers greater resistance to settling than the denser subrounded quartz grains. Q4A is a clastic unit different from the *in situ* growth and accumulation of carbonates characteristic of Q3, Q4B and Q5.

Q4B was dated as 180,000 B.P., and Q3 as 236,000 years B.P., so Q4A is of intermediate age. The Q3 surface was subaerially exposed developing as iron rich laminated crust and characteristic subaerial fabrics. The sea transgressed over Q3 depositing a transgressive lag, seen as rip up clasts in RH-5 (PLATE VI, Fig. 8), and coarse mollusc debris in RH-6. The clasts and the associated medium to coarse grain size indicate a high energy environment. Subsequently, the Q4A quartz bearing bioclastic unit was deposited. The medium to coarse grain size, and low angle laminations 15-17^{o}indicate a beach environment. Multer (1971) observed a 15^{o} dip on skeletal beachrock of Dry Tortugas, Florida. The Q4A topography was a low relief, almost horizontal unit, unlike the pronounced thickness variations within Q4B and Q5.

The multiple generation cement in Q4A is interpreted as a multistaged "marine" vadose cement of beachrock origin in part, succeeded by a meteoric vadose cement. The first generation micrite cement was a Mg-calcite or aragonite cement originally. Although this micrite evenly

rims most grains, it is occasionally thicker on the upper surfaces of grains. This suggests it was flushed in from above. Taylor and Illing (1971) observed similar cryptocrystalline cements in recent beachrocks of the Quatar Peninsula, Persian Gulf, interpreting them as reef derived muds flushed into the sands.

The 2nd generation rims of acicular cement are probably relict aragonite cements precipitated in a marine beachrock environment. The acicular nature of the cement is preserved locally where encased in sparry calcite cement of vadose origin. The calcite spar must have precipitated early in the vadose environment or the aragonite, unstable in meteoric conditions, would have been leached. The fibrous nature of the aragonite may have had a "baffle effect" on the distribution of percolating meteoric water, resulting in adjacent precipitation of calcite cements. Most of the calcate rims of Q4A are elongate crystals of low Mg-calcite spar with a similar thickness (100 μm) as the relict acicular cements. Perhaps this cement is an alteration of the original aragonite mineralogy to low Mg-calcite cement during vadose diagenesis. Land (1971) interpreted similar rims of low Mg-calcite form the Pleistocene Belmont Formation of Bermuda as beachrock cements altered to low Mg-calcite. Beachrock, common in recent environments, has rarely been recorded in ancient rocks; this

is a function of preservation. If relict aragonite is absent the low Mg-calcite rims are almost indistinguishable from similar rims precipitated in a meteoric phreatic lens.

Unlike the patchy distribution of vadose cements in Q5, Q4A cements form regular rims of cement around grains. Occasionally these cements show preferential crystal growth on the top or bottom of the grain. Similar cement distribution was noted by Taylor and Illing (1969) in a beachrock environment, where pores are filled with water and air indicative of a vadose environment, in this case a marine vadose environment. The evaporation of films of marine water around grains in an intertidal environment provides a mechanism for precipitation of aragonite or Mg-calcite cements (Multer, 1971) such as the acicular cements encased in calcite.

Most of Q4A porosity is secondary moldic porosity due to the dissolution of carbonate grains. A striking contrast exists in Q4A between areas with very high moldic porosity, and areas with abundant grains, well preserved primary texture and low porosity. Early diagenetic cements, in this case beachrock cement, protect the cemented grains from recrystallization and dissolution, explaining the porosity variability in Q4A. The protective nature of beachrock and other early cements has previously been recorded (Ginsburg, 1953; Multer, 1971 and Steinen, Harrison and

Mathews, 1973).

The combination of micrite cement with rims of acicular aragonite cement as discussed above has been observed in beachrock cements from Grand Cayman Island (Moore, 1971) and Gulf of Aquaba beachrocks (Friedman and Gavish, 1971).

Beachrock cementation requires stable sediment, supersaturation of aragonite in the pores and steep, well-drained beaches (Taylor and Illing, 1969). In core RH-2 a 15-17° inclination of bedding was observed. The filling of a pore requires 30,000 equivalent volumes of evaporated marine water (Evamy in Purser, 1973). The pumping mechanism required to flush this quantity of water through may be waves and tides (Taylor and Illing 1969). Low Mg-calcite cement precipitated in a meteoric vadose environment is the last cement to form, plugging intra-skeletal porosity. Evidence of quartz dissolution is common in Q4A. A pH of 9 to 9.5 is required for quartz dissolution (Friedman et al., 1976). Such high pH's have been measured in beachrock environments (Davies and Krinsley, 1973). The etched surfaces of the quartz grains and irregular embayments at the grain periphery noted in Q4A have been observed by Friedman et al. (1976) in beach-rock environments.

Exposed beachrock is commonly bored by algae

(Bathurst, 1976). Photosynthesis takes up bicarbonate ion and increases the pH, enhancing the precipitation of carbonate cement and the dissolution of quartz (Friedman, 1975).

The quartz grains are preferentially dissolved along dustlines and lines of inclusions. These lines are directions of weakness within the grain which are most readily dissolved when the grain is unstable at high pH's. There is no affinity between dustlines and the "boring" structures. These structures occur where dustlines are absent and may bifurcate, unlike dustlines. The "borings" are unlined, have parallel walls of fairly constant diameter (3-12 µm) and have a perpendicular to subperpendicular orientation to the grain surface. It is difficult to tell whether borings cut across micrite envelopes or were there prior to the micrite envelope formation. The scanning electron microscope reveals a solution-modified opening leading quickly into a borehole with circular cross-section (PLATE IX, Fig. B). Boreholes conform to the cylindrical shapes of the thalli (Golubic et al., 1975). Fungal borings tend to have smaller diameters than algal borings (Risk, person. commun.). However, Ostreobium quekettii, a photosynthetic algae found at depths from 1.5 m to 60 m in the Florida Keys, has diameters ranging 1-25 µm, commonly 2-5 µm (Lukas, 1974). The observed borings are 3-12 µm. Whether

PLATE IX SEM PHOTOS OF POTENTIAL BORINGS

Fig. A: RH-2 @ 31.5' (9.6m), 160 Magnification
The circle encloses a probable boring on the surface of a quartz grain. Notice the rounded surface of the grain implying fairly extensive transport and reworking. (scale = 100 μm)

Fig. B: RH-2 @ 31.5' (9.6m), 640 Magnification
A closeup of the above borehole reveals a solution enhanced entrance at the surface of the grain with a cylindrical borehole morphology recessed slightly. The quartz surface is extensively dissolved. The arcuate fractures may be solution enhanced, crescentic impact features. This dissolution of the quartz grain supports the suggestion that pH's greater than 9 have occured during deposition of this unit. (scale = 10 μm)

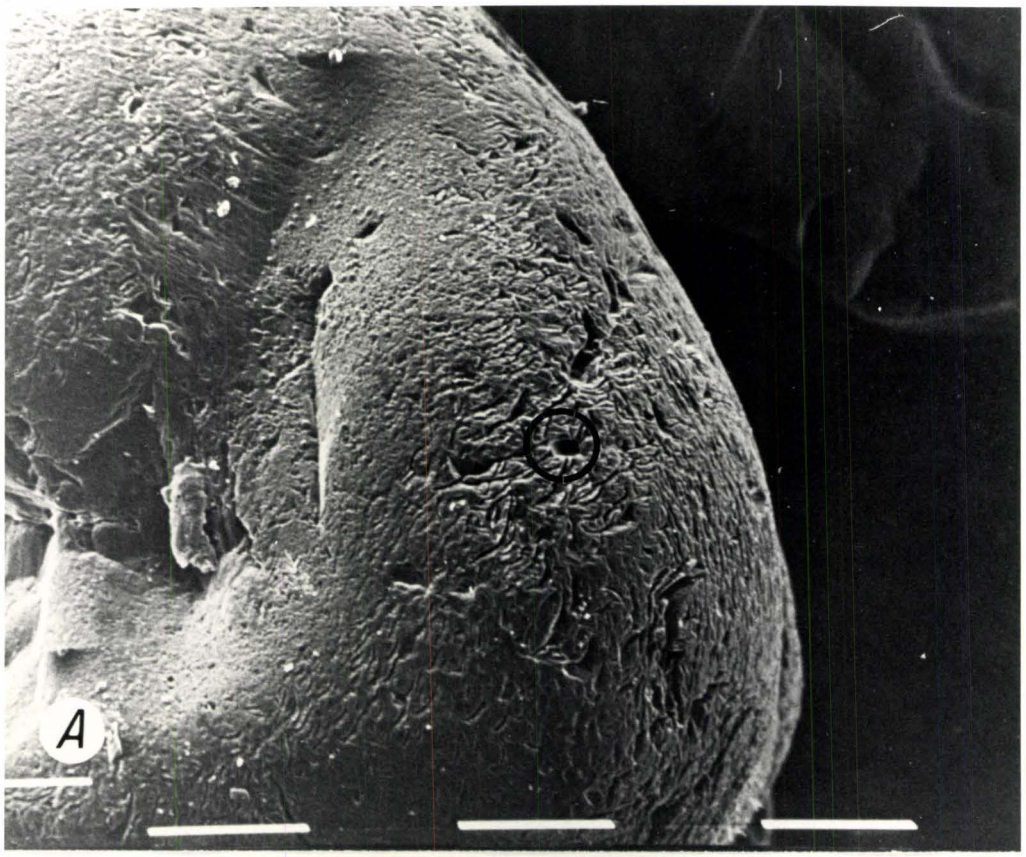
A

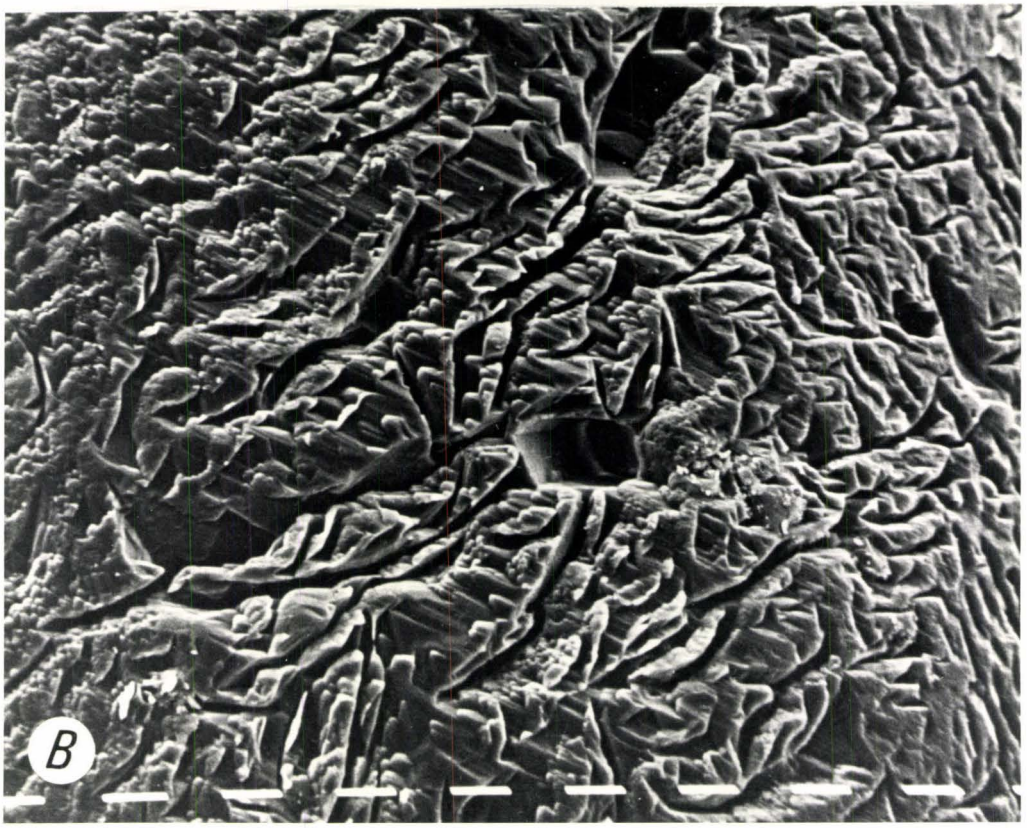
B

PLATE X PREFERENTIAL DISSOLUTION ALONG DUSTLINES IN QUARTZ Q4A

Fig. A: RH-2, slide #15 @ 27' (8.23m)
Dustlines and lines of inclusions transverse the subrounded quartz grain.

Fig. B: S.E.M. - RH-2, @ 31.5' (9.6m), 2500 Magnification
A fracture surface on a quartz grain reveals the unaltered appearance of dustlines which are vacuoles often filled with dust or liquid. These features are healed fractures which are directions of weakness in the crystal.

Fig. C: RH-2, slide #17, @ 30' (9.14m)
Preferential dissolution along the dustlines (direction of weakness) and subsequent precipitation of micrite has almost truncated the grain. Notice also, the irregular embayed periphery of the quartz grain.

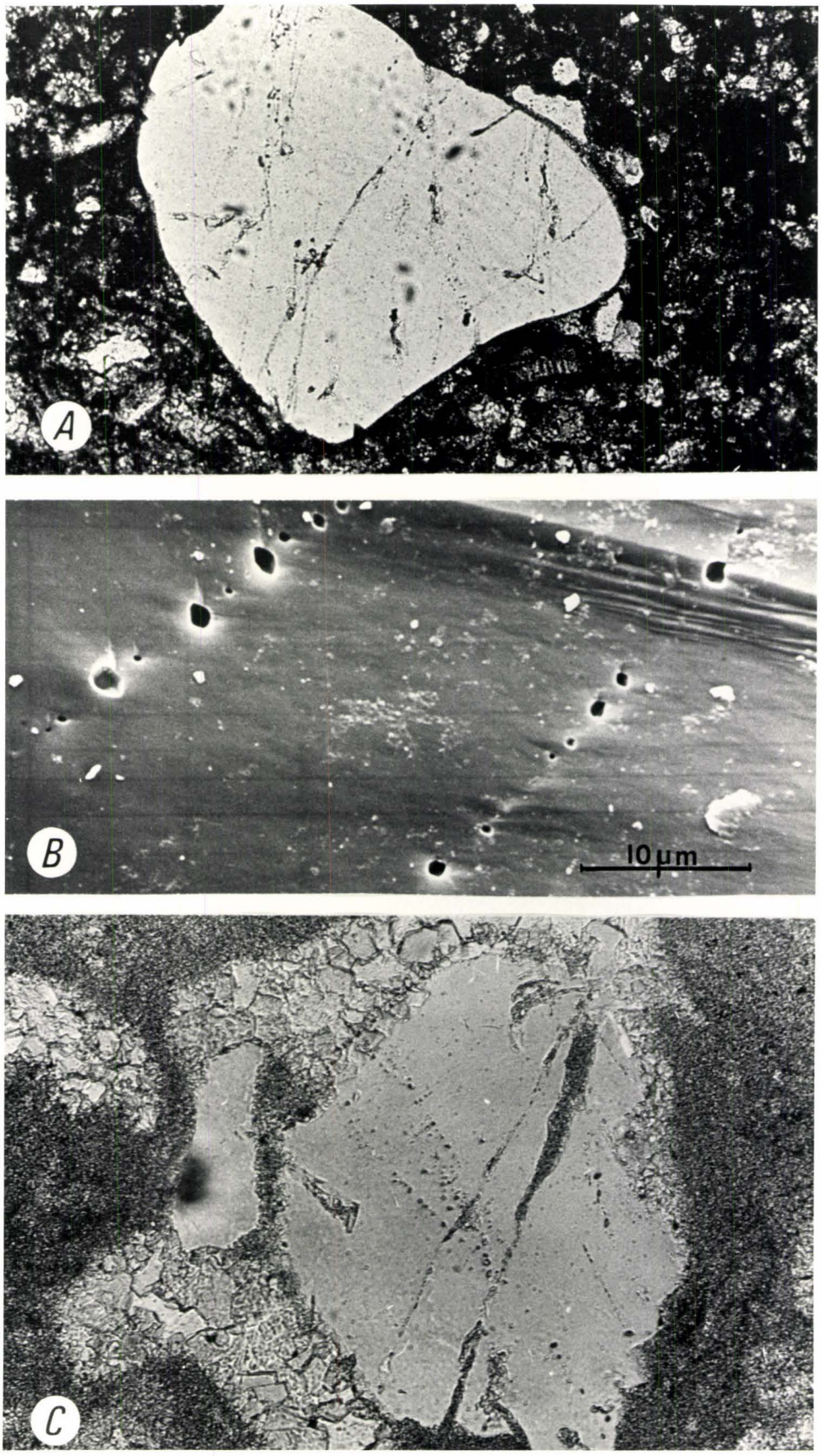
A
B
10 µm
C

these borings have a fungal or algal affinity is unknown. Jones and Goodbody (1982) have observed unlined borings with 2-12 µm diameters in glass fragments cemented into carbonate beachrock from Grand Cayman Island. These have been interpreted as algal, possibly Ostreobium which commonly bores the carbonate beachrock of the area.

Borers utilize a chemical process to attack the carbonate substrate exploiting directions of weakness, (i.e. cleavage) within the grain. It seems possible that the borers in Q4A are exploiting the quartz grains as a potential substrate when pH's greater than 9 render the quartz unstable. Jones and Goodbody suggest that high pH's may be a local phenomenon directly associated with algae (Jones and Goodbody, 1982).

6. LATE STAGE CEMENTS ASSOCIATED WITH VUGS AND CHANNELS

Observations

Euhedral bladed cements form botryoidal clusters around grains along some walls of vug and channel porosity. The dimensions of the blades range from 15 µm by 100 µm to 40 µm by 300 µm with low angle crystal terminations. The cements overlie grains and intergranular vadose equant spar that has been dissolved away to form the vugs. These cements have formed after the vadose spar which is the youngest cement. These cements are associated with a tan-orange stain that may vary locally in concentration. In RH-5 the orange stain is found in Q4B, at 4.4 m-6.4 m, in RH-6, Q5 at 0.30-1.2 m, near the present day sea level and in Q4B at 6.1-7.9 m. RH-7 has a blue-grey colored stain at 2.9-4.4 m, which is marbled throughout the carbonate matrix rather than directly related to vugs (PLATE XIII, Fig. B). Observing all 10 core recovered from the drilling program delineates a vague zonation of staining (Harrison, person. commun.). One zone is located 1.5 meters below the Q5/Q4B break in Q4B. Under SEM, it can be seen that a very fine grain material (clay?) has dusted the crystals, coating and rounding the terminations in part (PLATE XI, Fig. A,B). This dusting of material is the stain. Using

PLATE XI LATE STAGE BOTRYOIDAL CEMENTS

Fig. A: SEM RH-5 @ 18' (5.49m) 80 Magnification
Euhedral bladed cements with width 15-40 µm and length 100-300 µm, exposed along wall of channel porosity. The botryoidal nature of these cements is seen here. The blades radiate out from a shared nucleus. These cements are believed to be calcite cements deposited in a meteoric environment. (scale = 100 µm)

Fig. B: SEM RH-5 @ 18' (5.49m) 320 Magnification
Magnification of Fig. A. The crystals are dusted with a fine grain material that imparts an orange-brown stain to the cement. SEM probe analysis indicates a high iron content in this stain. (scale = 10 µm)

Fig. C: RH-5, slide #12 @ 18' (5.49m)
A thin section view of the bladed cements growing around a mollusc fragment, a part of the vug wall. Cross-polars.

Fig. D: RH-5, slide #12 @ 18' (5.49m)
A polarized thin section of the botryoidal radiating habit of these bladed calcite cements. Cross-polars.

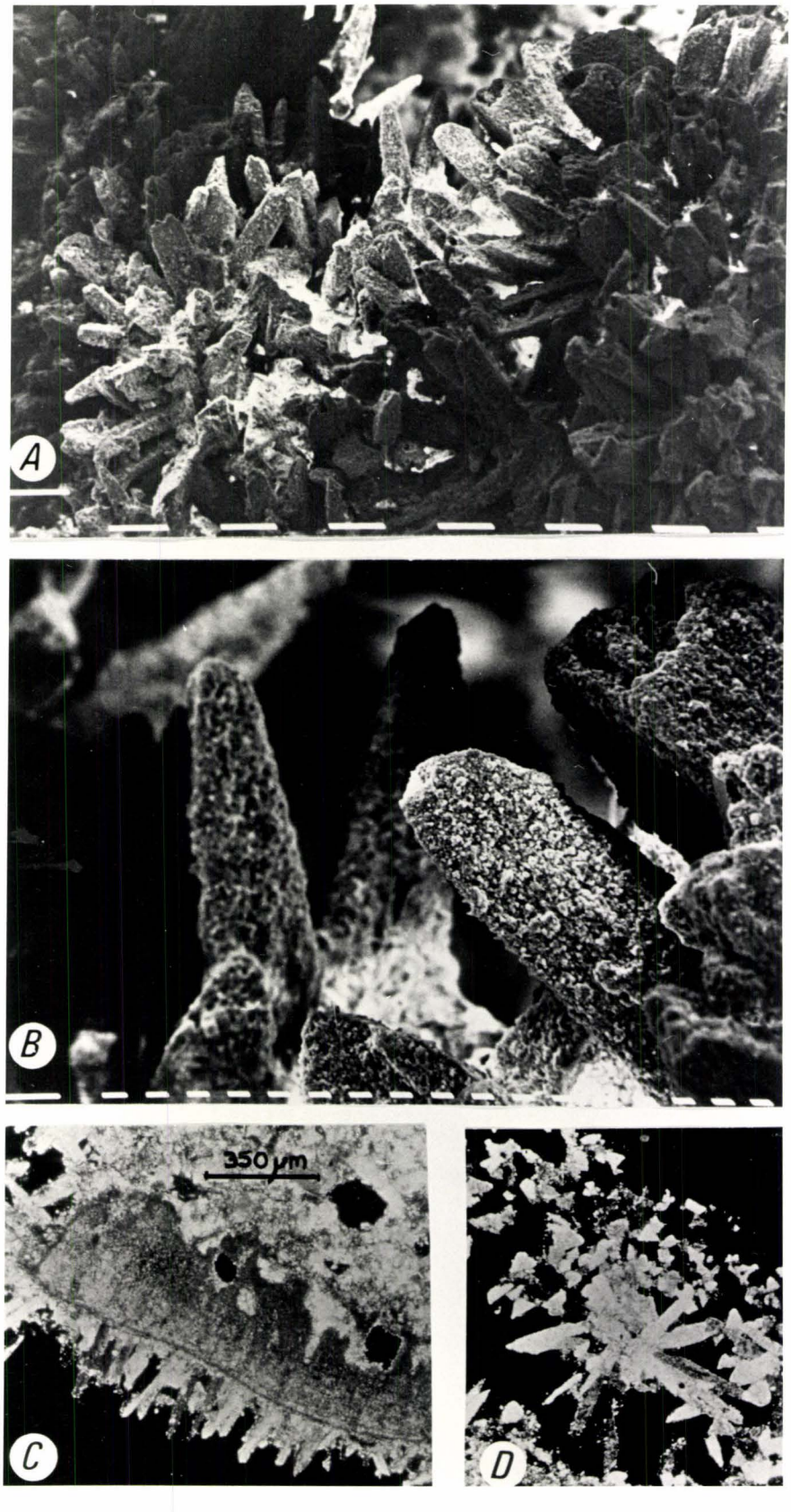
A
B
350 µm
C
D

a scanning electron probe, a chemical analysis of the tan-orange stain reveals the presence of Al, Cl, Ca, Sc, Co and large amounts of iron. The mottled blue-grey stain was found to have a similar composition, with an unusually high nickel content.

Discussion and Interpretation

The vugs and channels are secondary pathways of directed flow of meteoric water when intergranular porosity is plugged. A SEM sample along the exposed surface of a channel vug was observed to have extensive dissolution of calcite (PLATE XII, Fig. A,B). It appears these channels and vugs have alternating conditions favoring precipitation of low Mg-calcite bladed cements or of dissolution. Rainfall fluctuates daily and seasonally with most of the 152 cm annual rainfall occurring from June to October. A heavy rainfall may flush a large amount of water, undersaturated with respect to calcite through the vugs, resulting in dissolution. Alternatively, slow percolation of meteoric water would allow super-saturation of water with respect to calcite and subsequent precipitation of calcite cement. The bladed morphology of the cement suggests a low Mg-calcite cement precipitated in a meteoric phreatic environment. An alternative explanation is a vadose environment with ample water to provide films of water that produce bladed crystals with low angle termin-

PLATE XII VUGS

Fig. A: SEM, RH-6 @ 20.5' (6.25m), 320 Magnification
Calcite crystal terminations inside a vug.
(scale = 10 μm)

Fig. B: SEM, RH-6 @ 20.5' (6.25m), 320 Magnification
Extensive dissolution of the exposed calcite crystals due to the percolation of leaching solutions along the vuggy and channel porosity. (scale = 10 μm)

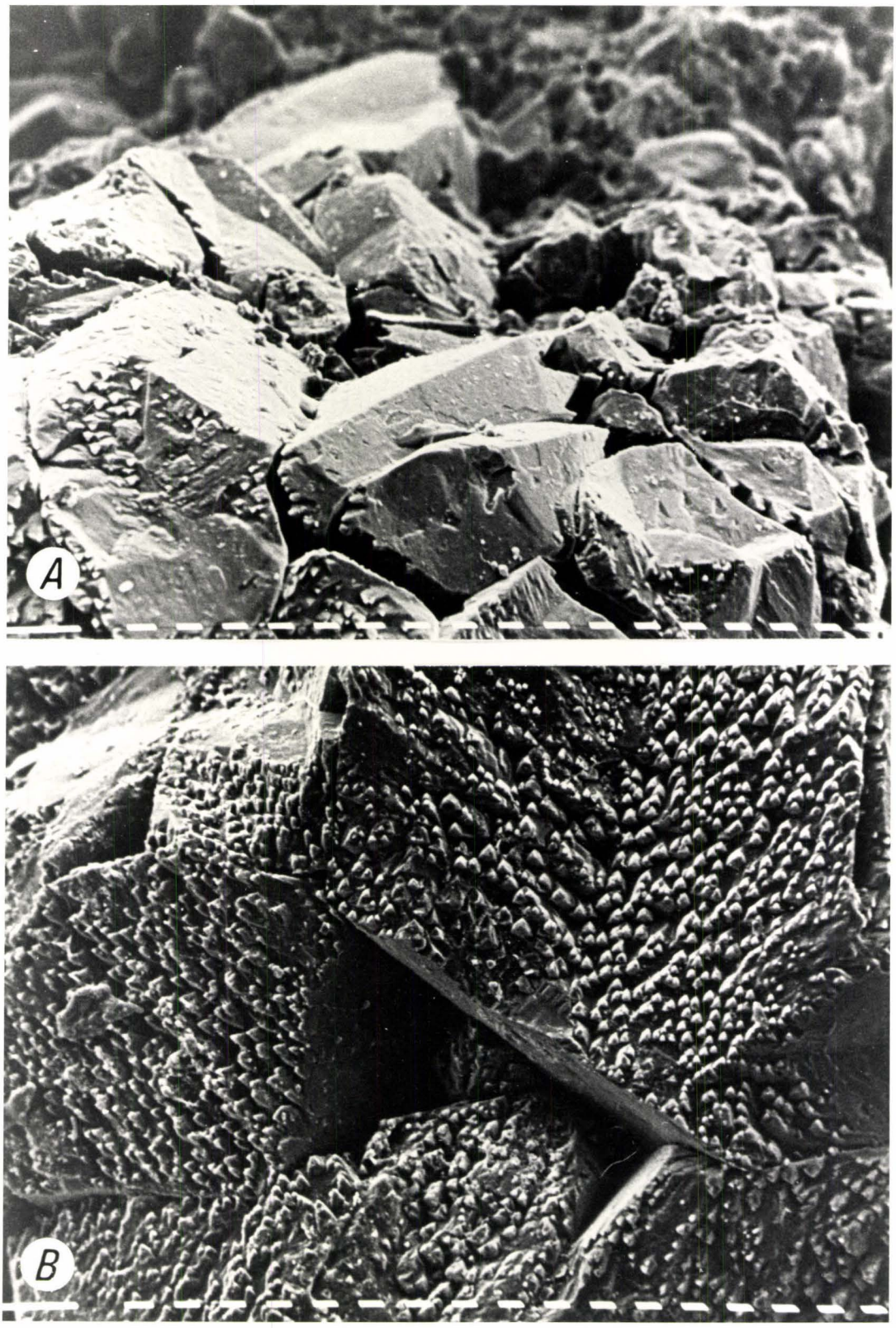
A
B

ations rather than meniscus cements with blunted terminations.

The stains are iron rich. The most obvious source of iron is the iron rich micrite associated with subaerial diagenesis at the surface. If this assumption is correct the stains associated with Q4B would have been dependent on the Q5/Q4B discontinuity surface, while the stains in Q5 are dependent on processes at the present day surface.

The unusually high nickel content of the blue-grey stain in RH-7 at 2.9-4.4 m may be due to scavenging of Ni from solution by iron.

This vague zonation of stains may be due to a zone of vugginess where directed channels allow percolating fluids to precipitate cements/stains. Therefore zonation might be controlled by the distribution of porosity. Alternatively the zonation may be due to an ephemeral meteoric phreatic lens. The existence of a permanent phreatic lens today is discredited, due to the highly porous nature of the rocks and the narrow width of the Key. The mixing by waves and storms probably reduces the perch effect of meteoric water on the denser marine water preventing a lens from forming. An ephemeral phreatic lens if present would have the dimensions of 40 feet (12.2 m) below sea level for every 1 foot (.3m) above sea level, according to the Ghyden Herzberg theory (Friedman, 1975).

PLATE XIII CORE

Fig. A: Modern Q5 surface with laminations and pockets of reddish brown subaerial micrite.

Fig. B: Well RH-7 (left to right)
Q5, 2' (.61m) a Halimeda rich sand.
Q4B, 13' (4.0m) vuggy zone with blue-grey stain.
Q4B, 18' (5.5m) vuggy porosity, probably controlled by solution enhancement of burrows.

Fig. C: Well RH-5
Q4B vuggy zone, from left to right
15.5' (4.7m) and 17.5' (5.3m) notice orange-brown stain associated with vuggy porosity
22.5' (6.9m) vuggy porosity
27' (8.2m) coral parially leached.

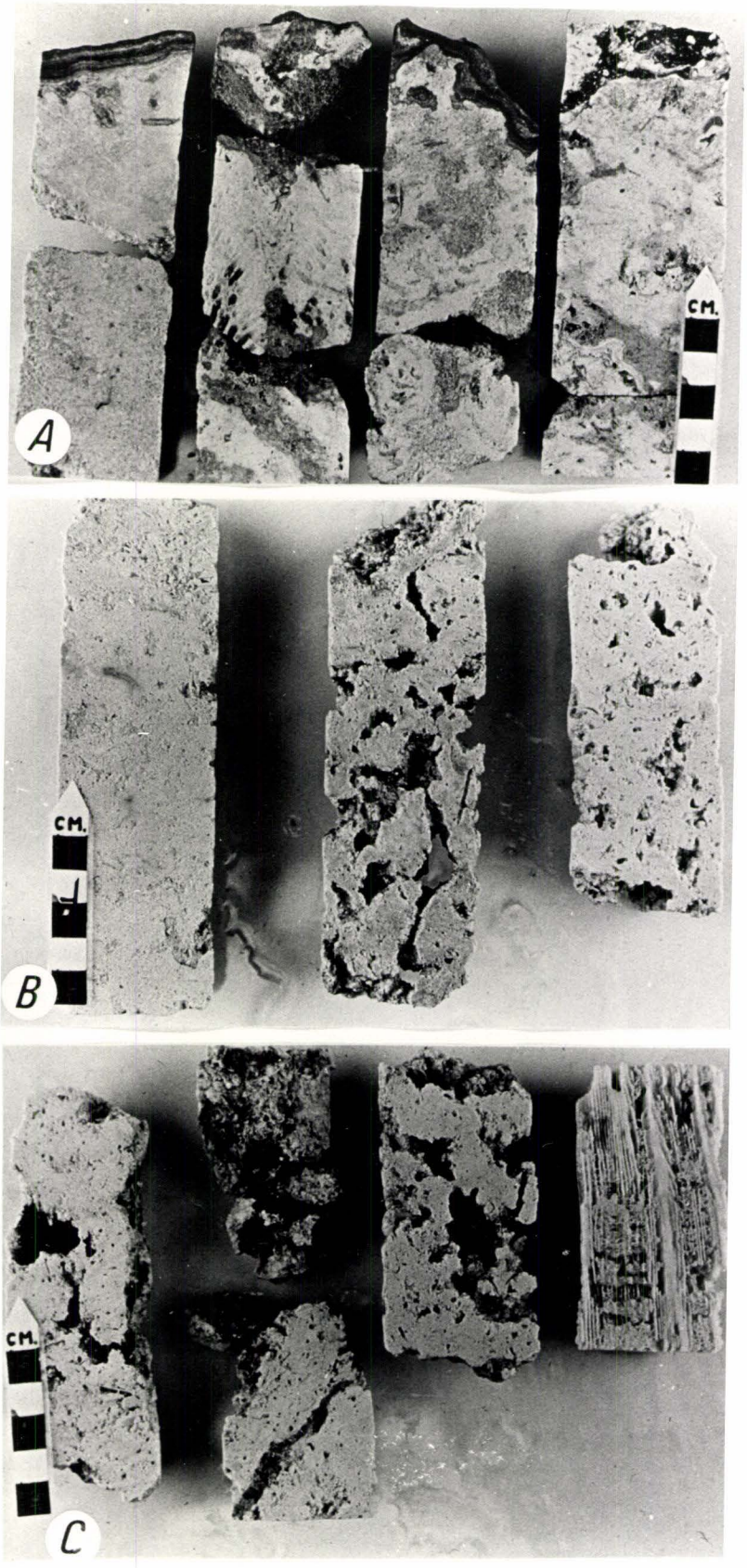
A
CM.
B
CM.
C
CM.

7. CONCLUSIONS

Q5 and Q4B are carbonate buildups of varying thickness. Q4A is a clastic quartz bearing unit, interpreted in part as a beachrock. Quartz dissolution indicates a pH greater than 9 during the deposition of Q4A. Of special interest in Q4A is the probably exploitation of a quartz substrate by endolithic borers.

Each unit is capped by subaerial exposure fabrics indicating shallowing upward cycles that coincide with Pleistocene eustatic sea level fluctuations. The multiple generation cements in Q4B suggest two periods of vadose exposure: one period after Q4B deposition at 180,000 B.P. and the other after the deposition of Q5 at 125,000 years B.P.. Q5 appears to lack diagenetic overprinting, having experienced a vadose environment exclusively. From petrographic study, solution enhanced interparticle porosity is the main porosity type for Q5, in contrast to moldic porosity for Q4B and Q4A. Aragonite is being leached in Q5, while Q4B and Q4A have completely altered to low Mg-calcite attesting to the advanced diagenetic maturity of Q4A and Q4B. The macroscopic vugs, observed in vague zones, are pathways of directed flow of percolating fluids, that precipitate late stage cements and stains or leach vug

walls. The vugs are non-fabric selective. Average total porosity remained constant for all units studied at 28.5%, and cements also remained constant at 27.5% total cement (Fig. 5). The majority of Q5 cement is autochthonous, and was derived from leached grains within Q5. Unit Q5 probably provided as allochthonous source of $CaCO_3$ in solution to Q4B during the 125,000 year emergence of Q5 and Q4B.

In carbonates, porosity is created, modified and ultimately destroyed (Pray and Choquette, 1970). Newly deposited carbonates may have as much as 40-70% porosity, in contrast to 0-2% porosity in ancient carbonates (Pray and Choquette, 1970). Potential hydrocarbon reservoir carbonates have 5-15% porosity. To retain porosity in these units, diagenesis (particularly cement precipitation) must have been arrested. The Key Largo limestone units Q4A, Q4B and Q5 of Pleistocene age are still very porous rocks (28.5% total porosity). By observing the progressive stabilization of such rocks, an understanding of how and why porosity is modified at intermediate stages of diagenesis may be deduced.

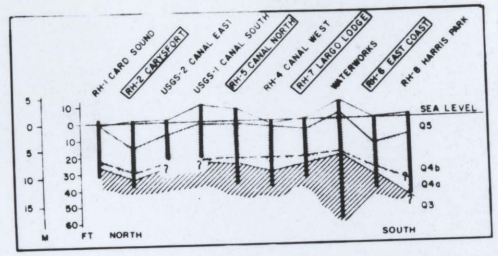

RH-2

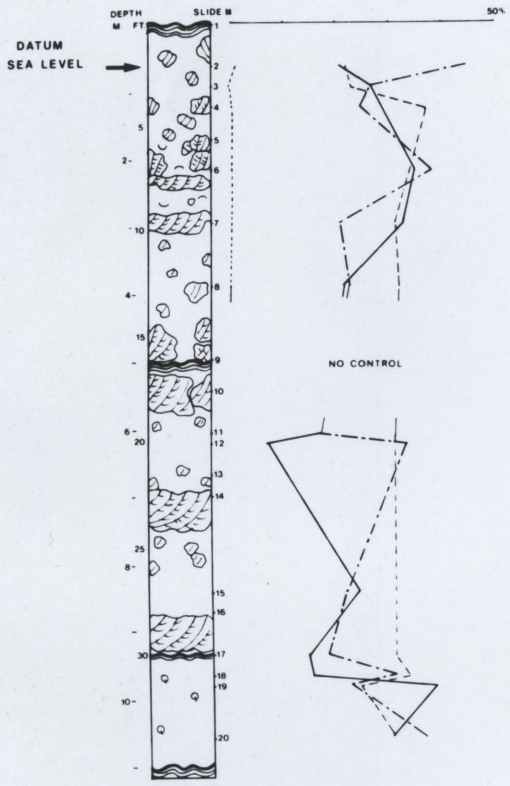

RH-5

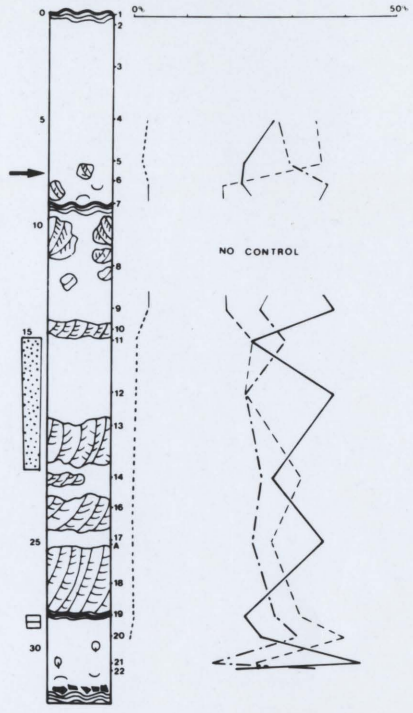

RH-7

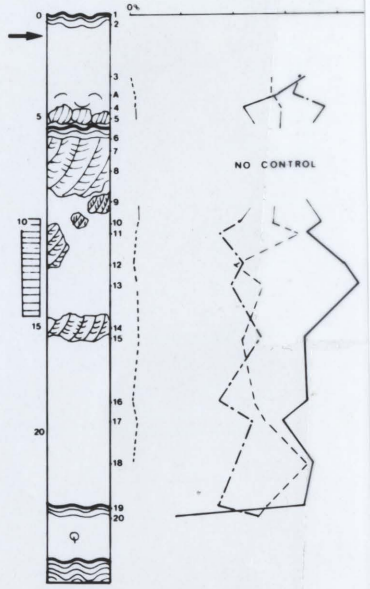

RH-6

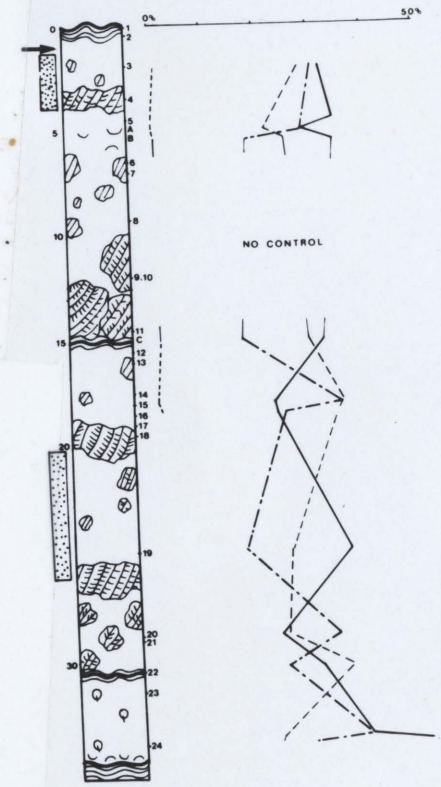

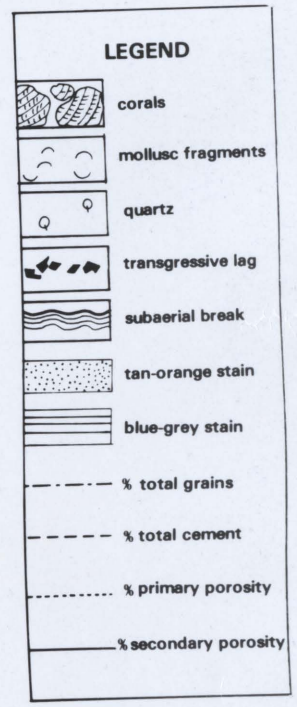

POINT COUNTING RESULTS vs. DEPTH IN CORE

Point counting values averaged for each unit

unit	%grains	%porosity	%2nd.porosity	%cement	%spar	%micr.	%env.	%matrix
Q5	29.70	28.48	27.64	27.78	21.06	2.84	3.88	14.80
Q4B	23.48	28.55	27.93	27.88	22.74	2.09	3.30	22.07
Q4A	26.37	29.06	29.40	27.36	22.08	3.54	1.76	19.11

Figure 5.

REFERENCES

Bathurst, R.G.C., 1976, Carbonate Sediments and Their Diagenesis, 2nd ed., Elsevier, Amsterdam, 658p.

Bricker, O.P., ed. 1971, Carbonate Cements, Johns Hopkins Press, Baltimore, Md., 376p.

Broecker, W.S. and Thurber, D.L., 1965, Uranium-series dating of corals and oolites from Bahaman and Florida Key limestones, Science, V. 149, p. 58-60.

Coniglio, Mario, 1981, Sedimentology of Pleistocene carbonates from Big Rine Key Florida, MSc. thesis, University of Manitoba, (unpubl.) p. 1-261.

Dunham, R.J., 1962, Classification of carbonate rocks according to depositional texture in Ham, W.E., ed., Classification of carbonate rocks, Amer. Ass. Petrol. Geol. Mem., no. 1, p. 108-121.

--------, 1971, Meniscus cement, in Bricker, O.P., ed., Carbonate Cements, Johns Hopkins Press, Baltimore, Md., p. 297-300.

Embry, A. and Klovan , Bull. C.S.P.G., V. 19, No. 4 (classification)

Enos, P., 1977, Part I, Holocene sediment accumulations of the south Florida shelf margin, in Enos, P. and Perkins, R.D., ed., Quaternary sedimentation in south Florida, Geol. Soc. Amer., Mem., no. 147, p. 1-130.

Evamy, B.D., 1973, The precipitation of aragonite and its alteration to calcite on the Trucial Coast of the Persian Gulf, in Purser, B.H. ed., The Persian Gulf, Springer-Verlag,N.Y., p. 329-341.

Friedman, G.M., 1964, Early diagenesis and lithification in carbonate sediments, J. Sediment. Petrology, V. 34, p. 777-813.

--------, 1975, The making and unmaking of limestones or the downs and ups of porosity, J. Sediment. Petrology, V. 45, No. 2, p. 379-398.

Friedman, Ali and Krinsley, 1976, Dissolution of quartz accompanying carbonate precipitation and cementation in reefs with an example from the Red Sea, J. Sediment. Petrology, V. 46, No. 4, p. 970-973.

Ginsburg, R.N., 1953, Beachrock in South Florida, J. Sediment. Petrology, V. 23, No. 2, p. 85-92.

Glover, E.D. and Pray, L.C., 1971, High Mg-calcite and aragonite cementation within modern subtidal carbonate sediment grains in Bricker ed., Carbonate Cements, Johns Hopkins Press, Baltimore, Md., p. 80.

Goulubic, S., Perkin, R.D., and Lukas, K.J., Boring microorganisms and microborings in carbonate substrates in Frey, R., ed., 1975, The Study of Trace Fossils, Springer-Verlag, N.Y., p. 229-259.

Halley, R.B., 1977, Estimating pore and cement volumes in thin section,

--------, and Harris, P.M., 1979, Fresh-water cementation of a 1,000 year-old oolite, J. Sediment. Petrology, V. 49, p. 969-988.

Harrison, R.S., 1975, Porosity in Pleistocene grainstones from Barbados: some preliminary observations, Bull. Can. Petrol. Geol., V. 23, p. 383-392.

-------- and Steinen, R.P., 1978, Subaerial crusts, caliche profiles, and breccia horizons: comparison of some Holocene and Mississippian exposure surfaces, Barbados and Kentucky, Geol. Soc. Amer., Bull., V. 89, p. 385-396.

Hoffmeister, J.E. and Multer, H.G., 1964, Pleistocene limestones of the Florida Keys, in Ginsburg, R.N., ed., Guidebook Field Trip no. 1, Geol. Soc. Amer., p. 57-61.

-------- and Multer, H.G., 1968, Geology and origin of the Florida Keys, Geol. Soc. Amer., Bull., V. 79, p. 1487-1505.

James, N.P., 1974, Diagenesis of scleractinia corals in the subaerial vadose environment, J. Paleontol., V. 48, p. 785-799.

Jones, B., and Goodbody, Q.H., 1982, The geological significance of endolithic algae in glass, (in press) Canadian J. Earth Sciences

Klappa, C.F., 1979, Calcified filaments in Quaternary calcretes: organo-mineral interactions in the subaerial vadose environment, J. Sediment. Petrology, V. 49, p. 955-968.

Land, L.S., 1967, Diagenesis of skeletal carbonates, J. Sediment Petrology, V. 37, p. 914-930.

--------, 1971, Phreatic vs. meteoric diagenesis of limestones, evidence from a fossil water table in Bermuda in Bricker, O.P., ed., Carbonate Cements, Johns Hopkins Press, Baltimore, Md., p. 133.

Lindholm, R.C. and Finkelman, R.B., 1972, Calcite staining, semiquantitative determination of ferrous iron, J. Sediment. Petrology, V. 42, p. 239-242.

Longman, Mark W., 1980, Carbonate diagenetic textures from near surface diagenetic environments, AAPG Bulletin, V. 64, No. 4, p. 461-487.

Lukas, K.J., 1974, Two species of the chlorophyte genus Ostreobium from skeletons of Atlantic and Caribbean Reef corals, J. of Phycology, V. 10, p. 331-335.

Milliman, J.D., 1974, Marine Carbonates, Springer-Verlag, New York, N.Y., 375 p.

Mitterer, R.M., 1975, Ages and diagenetic temperatures of Pleistocene deposits of Florida based on isoleucine epimerization in Mercenaria, Earth Planet. Sci. Lett., V. 28, p. 275-282.

Moberly, Ralph, 1973, Rapid chamber filling growth of marine aragonite and Mg-calcite, J. Sediment. Petrology, V. 43, No. 3, p. 634-635.

Moore, C.H.Jr., and Billings, G., 1971, Model of Beachrock cementation, Grand Cayman Island, B.W.I. in Bricker, O.P., ed., Carbonate Cements, Johns Hopkins Press, Baltimore, Md., p. 133.

Muller, G., 1971, Gravitational cement: An indicator for the vadose zone of the subaerial diagenetic environment in Bricker, O.P., ed., Carbonate Cements, Johns Hopkins Press, Baltimore, Md., p. 301.

Multer, H.G. and Hoffmeister, J.E., 1968, Subaerial laminated crusts of the Florida Keys, Geol. Soc. Amer., Bull., V. 79, p. 183-192.

--------, 1971,Holocene cementation of skeletal grains into beachrock, Dry Tortugas, Florida in Bricker, O.P., ed., Carbonate Cements, Johns Hopkins Press, Baltimore, Md., p. 25.

--------, 1977, Field Guide to Some Carbonate Rock Environments of the Florida Keys and Western Bahamas, Kendall/Hunt Publishing Comp., Iowa.

Perkins, R.D., 1977, Part II, Depositional framework of Pleistocene rocks in south Florida, in Enos, P. and Perkins, R.D., ed., Quaternary sedimentation in south Florida, Geol. Soc. Amer., Mem., no. 147, p. 131-198.

Pingitore, N.E.Jr., 1971, Submarine precipitation of void-filling needles in Pleistocene Coral, in Bricker, O.P., ed., Carbonate Cements, Johns Hopkins Press, Baltimore, Md., p. 68.

Pingitore, N.E., 1976, Vadose and phreatic diagenesis: processes, products and their recognition in corals, J. Sediment. Petrology, V. 46, p. 985-1006.

Pittman, E.D., 1974, Porosity and permeability changes during the diagenesis of Pleistocene corals, Barbados, West Indies, Geol. Soc. Amer., Bull., V. 85, p. 1811-1820.

Pray, L.C. and Choquette, P.W., 1970, Geologic nomenclature and classification of porosity in sedimentary carbonates, Amer. Assoc. Petrol. Geol., Bull., V. 54, p. 207-250.

Scholle, P.A., 1978, Carbonate rock contituents, textures, cements and porosities, Amer. Assoc. Petrol. Geol., Memoir 27, Tulsa Oklahoma.

Stanley, S.M., 1966, Paleoecology and diagenesis of Key Largo Limestone, Florida, Amer. Assoc. Petrol. Geol., Bull., V. 50, p. 1927-1947.

Steinen, R.P., Harrison, R.S., and Matthews, R.K., 1973, Eustatic low stand of sea level between 125,000 and 105,000 B.P.: evidence from the subsurface of Barbados, West Indies, Geol. Soc. Amer., Bull. V. 84, p. 63-70.

Steinen, R.P., 1974, Phreatic and vadose diagenetic modification of Pleistocene limestone: petrographic observations from subsurface of Barbados, West Indies, Amer. Assoc. Petrol. Geol., Bull., V. 58, p. 1008-1024.

Stoddart, D.R. and Cann, J.R., 1965, Nature and origin of beachrock, J. Sediment. Petrology, V. 35, p. 243-246.

Taylor, J.C. and Illing, L.V., 1969, Holocene intertidal calcium carbonate cementation, Qatar, Persian Gulf, Sedimentology, V. 12, p. 69-107.

Taylor, J.C.M. and Illing, L.V., 1971, Variation in recent beachrock cements, Qatar, Persian Gulf, in Bricker, O.P., ed., Carbonate Cements, Johns Hopkins Press, Baltimore, Md., p. 32-35.

Wehrfritz, W., 1973, Quartz grain texture: a study of the surface texture of intertidal sand grains with a scanning electron microscope, Tech. Memo 73-8, unpublished, McMaster University.

APPENDIX A

Procedure

Two inch core from four wells was logged to the Q3 surface encompassing units Q5, Q4B and Q4A. From north to south along Key Largo the wells were logged to the following depths: RH-2 35.5', RH-5 32.5', RH-7 26.5' and RH-6 34.5'. The core and thin-sections were originally measured in feet. For accuracy, the locations of thin sections and samples will be given in feet for the Appendix. Throughout the text, these values have been converted to metric units.

Point Counting

Three hundred points were counted at systematic intervals across the slide for 50 thin-sections at 10X, delineating: grains, primary porosity, secondary porosity, matrix, sparry cement, micrite cement and micrite envelopes. For point counting, thin sections were taken 2-3 feet (0.6-0.9m) below the Q5 and Q4B discontinuity surfaces in order to avoid subaerial fabrics associated with these surfaces, this was not done for Q4A since this break had not previously been established.

For unit Q5 it was the author's decision to include interparticle porosity as solution enhanced secondary

porosity. For Q4A, even rims of micrite with sharp inner contacts to adjacent grains were classified as micrite cement. Irregular inner contacts suggested an affinity with micrite envelopes and were classified as such.

The point counting data was converted to percentages for each slide and tabulated:

RH-2

Slide #	Depth (feet)	# Points	% Total Grains	% Poro-sity	Prim. Poro-sity	2nd. Poro-sity	Total Cement	Spar	Micrite	Env.	Matrix	
2	2	264	45.5	22.3	1.1	21.2	21.5	17.0	3.4	1.1	10.6	
3	3	301	26.9	26.9	-	26.9	22.6	19.9	-	2.7	23.3	
4	4	296	25.0	29.4	.34	29.1	36.8	26.0	4.4	6.4	8.8	Q5
6	7	350	38.3	36.0	.57	35.4	33.7	28.9	1.4	3.4	10.3	
7	9.5	354	20.9	33.4	.3	33.1	30.5	24.0	2.0	4.5	15.3	
8	12.5	292	22.9	21.9	-	21.9	31.9	26.7	1.4	3.8	23.3	
11	19.5	267	17.2	17.6	-	17.6	30.7	27.7	.75	2.2	34.5	
12	20	357	33.6	7.8	-	7.8	31.0	28.0	.6	2.5	27.5	Q4B
15	27	389	22.0	24.6	.3	24.3	30.8	25.6	-	5.2	22.5	
17	30	390	18.5	14.9	-	14.9	31.0	28.2	2.3	0.5	35.1	
18	31	375	31.5	15.5	-	15.5	33.8	26.1	6.7	1.0	19.2	
19	31.5	375	22.7	38.9	-	38.9	24.3	19.2	3.2	1.9	14.1	Q4A
20	34	348	37.0	30.2	-	30.2	31.7	23.6	4.9	3.2	1.1	

Env. = envelope

Slide #	Depth (feet)	# Points	% Total Grains	% Poro-sity	Prim. Poro-sity	2nd. Poro-sity	Total Cement	Spar	Micrite	Env.	Matrix	
4	5	262	27.9	29.4	2.7	26.7	34.4	19.5	14.9	-	8.4	
5	7	311	29.9	22.8	1.9	20.9	35.4	19.6	2.9	12.9	11.9	Q5
6	8	236	36.9	23.3	3.0	20.3	16.5	16.1	.42	-	23.3	
9	14	300	24.1	41.3	3.3	38.0	17.6	15.3	2.3	-	17.0	
11	15.5	244	29.1	23.7	0.82	22.9	22.1	21.3	0.8	-	25.0	
12	18	269	21.5	39.0	0.74	38.3	21.2	21.2	-	-	18.2	Q4B
14	22	305	24.3	27.2	0.33	26.9	31.5	31.1	.33	-	17.0	
A	25	320	22.8	36.9	0.30	36.6	25.6	17.5	3.8	4.4	14.7	
19	28.5	211	27	22.3	0.5	21.8	30.8	29.4	1.4	-	19.9	
20	29.5	284	31.3	24.6	-	24.6	39.4	27.5	10.9	1.1	4.6	Q4A
21	30.8	340	15.6	44.1	-	44.1	22.9	19.1	2.4	1.5	17.4	
22	31	349	34.7	20.1	-	20.1	23.2	22.6	-	0.6	22.1	

Env. = envelope

Slide #	Depth (feet)	# Points	% Total Grains	% Poro- sity	Prim. Poro- sity	2nd. Poro- sity	Total Cement	Spar	Micrite	Env.	Matrix	
3	3	343	32.1	33.8	-	33.8	27.1	20.4	1.17	5.5	8.5	
A	3.8	280	30.4	28.6	0.4	28.2	27.1	23.9	0.7	2.5	13.2	Q5
4	4.5	235	37.0	22.1	0.4	21.7	28.8	23.4	2.1	3.4	11.9	
10	10	309	20.7	37.9	1.6	36.2	27.2	15.2	7.4	4.5	12.6	
11	10.5	222	17.1	34.7	0.9	33.8	32.0	24.3	4.5	3.2	16.2	
12	12	319	21.6	40.8	0.3	40.4	19.7	15.4	1.9	2.5	17.9	
13	13	293	19.1	44.4	1.0	43.3	24.9	18.8	2.7	3.4	11.6	Q4B
15	15.5	332	24.7	34.0	1.2	32.8	20.8	18.1	1.5	1.2	20.5	
16	18.5	343	16.3	33.8	-	33.8	22.7	20.4	1.2	1.2	27.1	
17	19.5	366	22.4	29.0	0.3	28.7	25.1	22.1	1.6	1.4	18.6	
18	21.5	311	19.6	34.1	-	34.1	33.1	26.4	4.2	2.6	12.9	
19	23.5	239	15.9	32.6	-	32.6	25.1	18.4	5.0	1.7	26.4	
20	24	303	23.8	7.9	-	7.9	23.8	20.8	2.0	1.0	44.6	Q4A

Env. = envelope

Slide #	Depth (feet)	# Points	% Total Grains	% Poro-sity	Prim. Poro-sity	2nd. Poro-sity	Total Cement	Spar	Micrite	Env.	Matrix	
3	2	326	30.1	32.5	0.6	31.9	28.1	20.2	2.1	5.8	9.2	
5	4.5	226	28.7	34.1	-	34.1	22.6	14.2	2.2	6.2	14.6	
A	5	347	28.2	28.8	-	28.8	21.6	15.6	3.2	2.9	21.6	Q5
B	5.5	351	17.9	34.5	0.3	34.2	25.1	20.5	1.1	3.4	22.5	
C	15.0	328	16.1	31.7	-	31.7	28.7	27.1	0.9	0.6	23.5	
15	18.0	338	34.4	23.0	0.89	22.2	35.2	26.3	1.5	7.4	7.4	
16	18.5	366	24.1	23.0	0.27	22.7	34.1	25.4	3.0	5.7	18.9	
19	25,0	286	16.7	37.4	1.0	36.4	24.8	15.7	2.8	6.3	21.0	Q4B
21	29.0	313	33.6	22.7	-	22.7	23.6	14.7	2.2	6.7	20.1	
22	30.5	325	23.6	30.6	-	30.6	35.8	21.5	8.7	5.6	10.1	
24	33.8	327	39.0	39.	-	39.0	22.0	21.3	-	0.7	-	
25	34.0	316	28.1	50.5	-	50.5	21.4	21.4	-	-	-	Q4A

Env. = envelope

APPENDIX B

Samples and Methods

Descriptive Petrography

Forty-seven thin sections from wells RH-2 and RH-5 were described in detail using a polarizing microscope. RH-2 and RH-6 have a finer overall grain size than RH-5 and RH-7. As a result, one of each was selected to account for possible diagenetic differences due to grain size. Systematic descriptions of these slides and of logged core are available through Dr. Mike Risk, McMaster University.

X-ray Diffraction

Two coral samples from: Q5 RH-6 @ 10.5' and Q4B RH-2 @ 22.5' (Montastrea annularis) were tested for the persistence of aragonite. The corals were ground to a fine powder, quartz was added to calibrate the d-spacings of the crystal peaks. Both samples had completely altered to calcite.

Stains

Twenty-one hand specimens were stained to determine if the calcite cements contained ferrous iron. The hand specimen was etched in a 2% HCl solution (998ml distilled water, 2ml concentrated HCl) for 20 seconds. The sample was rinsed in running distilled water then immersed in the staining solution for 4 minutes, at 25°C. The stain con-

tained: 1 gm alizarin red-S and 5 gm potassium ferrocyanide in 1 liter of .2% HCl solution (98 ml distilled H_2O, 2 ml HCl)(Lindholm and Finkelman, 1971). Calcite stains red and iron stains purple to blue. The stain was first tested on the ferroa n calcite cement of an ammonite to certify its effectiveness.

Sample locations for stains:

RH-2 depth (ft.)	RH-5 depth (ft.)	RH-6 depth (ft.)
2.5	3.5	*31
5.5	7	
9.5	8	
12	9	
19	12	
22.5	14	
*27	20.8	
29.5	21.3	
*31.5	23.3	
*35	*30	

*blue stain due to yellow metallic mineral (FeS_2) associated with the quartz, all other samples stained red

Scanning Electron Microscopy

The carbonate was dissolved in a 10% HCl solution. The solution was filtered using a vacuum pump filter leaving a quartz residue. The quartz grains were mounted on SEM stubs, observed and photographed on a scanning electron microscope using 20-2,500x magnifications. The quartz

samples were taken from Q4A: RH-6, 31' and RH-2, 31.5'.

Sections of vug walls with botryoidal cements and stains were cut and mounted on SEM stubs, observed and photographed.

Samples of cements and stains:

Well	depth (ft.)	
RH-6	20.5	botryoidal cement
RH-6	11.5	botryoidal cement
RH-2	35	botryoidal cement
*RH-5	28	blue-grey stain
*RH-5	18	orange stain
RH-5	10	tan/orange stain

*SEM probe analysis was conducted on these samples.

Results of SEM chemical analysis:

RH-5 18' Orange stain bladed botryoidal cement, nine analyses were run for this sample, the followimg results are from 1 representative sample:

Element	Centroid	Area	
Al	1.39	305.03	(± Al and Co)
Cl	2.52	908.99	
Ca	3.60	16151.00	
Sc	3.92	2374.00	
Fe	6.29	1319.95	
Co	6.90	111.84	

RH-5 @ 28', Blue-grey stain, 3 analyses were run for this sample.

Element	Centroid	Area
Ca	3.69	27809.98
Sc	4.02	3145.62
Fe	6.40	397.60
Ni	7.47	30.21